Cellular Subscriber Lines (CSL): A Wireless-Wireline Physically Converged Architecture

John M. Cioffi, *Fellow, IEEE*, Chan-Soo Hwang, *Senior Member, IEEE*, Ioannis Kanellakopoulos, *Fellow, IEEE*, Jisung Oh, *Member IEEE*, and Ken J. Kerpez, *Fellow, IEEE*

(Invited Paper)

***Abstract*— Wireless-wireline convergence and cellular wireless deployment can economically accelerate through partial transmission of wireless 4G, 5G (generally 3GPP-standards-compliant), and/or Wi-Fi 6 baseband signals on the billions of copper phone, Ethernet, coaxial cable, and other wireline connections. This article poses such a Cellular Subscriber Lines (CSL) re-use architecture and investigates large bandwidth-efficiency gains, as well as the consequent cost-efficiency improvement that accrues for CSL's deployment infrastructure. In-home wireless signals' seamless distribution partially over copper links can achieve good data-rate-versus-distance profile. Results here also expand to Wi-Fi (possibly with MIMO use) on Ethernet multi-pair cables, finding very large gains over existing enterprise mesh (ad-hoc or otherwise) approaches.**

***Index Terms*— Communication channels, communication system planning, modular computer systems, multidimensional systems, multiplexing, radio communication, radio repeaters, resource management.**

I. Introduction

CELLULAR wireless standards' advance[1] through the last 15 years' 3GPP releases to current (5G) releases has leveraged well the multicarrier modulation methods deployed in earlier DSL networks. This advance includes also wireless' Multiple-Input-Multiple Output (MIMO) and MU-MIMO (MU=multi-user) signal processing that followed Digital Subscriber Line's (DSL's) vectoring methods, particularly for large numbers of antennas. This synergy suggests the potential **direct** use of wireless baseband-modulation methods on copper wireline connections, extended through frequency heterodyning at the customer's premises for connection to/from desired wireless end-devices. This article's work expands upon the innovative wireless-over-cable work of Gambini, Spagnolini and their colleagues, pioneered in [1]–[4] and more recently updated to current multiple-antenna expectations and consequent spectral-spatial trade-offs in [5]–[7]. This article's expanded new work circumvents some of these earlier works' spectral-spatial resource-allocation issues. The new proposed alternatives introduce cloud-based management and target more recent wider-frequency-band MIMO cellular and Wi-Fi transmission systems' use with a frequency-scaled time-division burst-mode sharing of wireline connections. This article suggests exploitation, rather than circumvention, of newer cellular and Wi-Fi methods' significant inherent MIMO processing. The proposed new methods also help improve upon the pioneering work and products by multiple authors/inventors of Ericsson's "Radio-Dot Systems" in [8]–[10], particularly addressing duplexing and multi-user-multiplexing issues. The new methods offer improvements over these earlier methods' remote radio units for both single-pair and multi-pair wireline connections. In responding to the Editor-in-Chief's invitation to project future copper-wireline technologies' path,[2] the authors here chose to explore this wireless-wireline convergence path for copper's future projections because it offers many economic and performance advantages as copper-link lengths decrease and wireless systems advance in a convergent telecommunications' world.

Cellular wireless standards' coded-OFDM[3] methods can exhibit only small performance loss on copper with respect to the related DMT[4] methods developed and optimized specifically for copper. These wireless methods' resulting performance is good if cellular's wireless **modulation-coding-scheme (MCS)**parameters and channel selection are properly activated and used, as in Section II of this article. Further, Section III shows that exploitation of existing wireless

Manuscript received November 2, 2019; revised February 15, 2020, May 6, 2020, and July 7, 2020; accepted August 19, 2020. Date of publication September 1, 2020; date of current version December 16, 2020. The associate editor coordinating the review of this article and approving it for publication was L. Wei. *(Corresponding author: John M. Cioffi.)*

John M. Cioffi is with the Department of Electrical Engineering, Stanford University, Stanford, CA 94305 USA, and also with ASSIA Inc., Redwood City, CA 94065 USA (e-mail: cioffi@stanford.edu).

Chan-Soo Hwang is with Technology Office, ASSIA, Inc., Redwood City, CA 94065 USA.

Ioannis Kanellakopoulos is with Oraton Consulting, Redwood City, CA 94065, and also with ASSIA, Inc. (Consultant), Redwood City, CA 94065 USA.

Jisung Oh is with the Department of Wireless Engineering, ASSIA Inc., Redwood City, CA 94065 USA.

Ken J. Kerpez is with ASSIA Inc., Redwood City, CA 94065 USA.

Color versions of one or more of the figures in this article are available online at https://ieeexplore.ieee.org.

Digital Object Identifier 10.1109/TCOMM.2020.3020572

[1]Use of the term "3GPP "here corresponds to a series of wireless standards in 4G, 5G, and the future by the 3GPP (3rd Generation Partnership Project) standards group associated with the International Telecommunications Union Standards Organization, see for instance [22].

[2]Rather than dual wireline-only standards' path well described for instance in [48], [49].

[3]OFDM = Orthogonal Frequency Division Multiplexed, see for instance [23].

[4]DMT = Discrete MultiTone, see [26].

baseband MIMO and MU-MIMO systems leads to additional improvement. Section IV further shows the proposed methods can simplify so-called "mesh" or "multi-access-point (MAP)" wireless deployments' range and efficiency. Indeed, these cellular-wireless, or Wi-Fi-wireless, MCS and MIMO methods' re-use on copper can lead to many improvements in cost, in infrastructure leverage, and in acceleration of wireless residential networks' economically profitable deployment; these same benefits were also generally noted in [1]–[10]. This article also investigates a related architecture that exploits the existing enterprise Ethernet cable infrastructure, advancing performance with respect to [9], [10].

There are globally more than 1 billion residential twisted-pair wireline connections, which form an infrastructure that can facilitate wireless "mini-tower" deployment. Many of these wireline connections have shortened copper links as fiber deployment increasingly migrates closer to the customer premises. The last copper link's replacement with fiber, however, is extremely expensive, because fiber's high construction costs then incur for only one customer. Substitution of wireless transmission for wireline transmission becomes most attractive with smaller cell size, and so substitution of wireless for copper/fiber has range limits. When fiber reaches a building's basement, wireline twisted pairs – or in some cases a single home-run coax cable – can complete the connection to multiple dwelling units because those interior copper links to residential living units already exist. By contrast, in-building fiber-installation costs can be unacceptably high or may violate construction laws and need special permits (or be physically or aesthetically impossible [11]). From an expanded wireless-deployment perspective, cellular's wireless transmissions – especially as carrier frequencies increase – have problems penetrating building walls. The copper links already penetrate the walls and were typically installed at the building's initial construction. 3GPP/5G New Radio (NR) standards releases' even higher millimeter-wave carrier frequencies are even less effective at penetrating walls, and thus wireless network service providers otherwise face an increased infrastructure cost to build more cell towers closer to end-devices, or to place their equivalents inside buildings or rooms. Additionally, the copper wireline connections allow power delivery from either end of the wire to the other, eliminating the possible issue of no power at a cell site (or conversely removing the need for local batteries to ensure service continuity inside a building). All these performance and economic efficiency possibilities encourage and motivate this CSL work.

Better security is a further advantage of any approach that uses wires into the home before launching wireless service within the home. Better security arises because the signals outside the home are therefore less available to an eavesdropper or attacker.

Figure 1 illustrates such a "**CSL** system" conceptually, superimposing the copper twisted-pair line structures on a popular "massive-MIMO-style" diagram. As the name implies, this is more cellular than a DSL[5] system, except that cellular

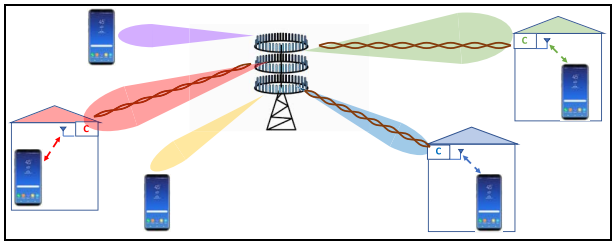

Fig. 1. Illustration of CSL as superimposed upon a massive MIMO system.

wireless signals are carried for a link portion on ordinary telephone wires. Such a system leverages the increasing and much larger penetration and global use of cellular wireless radio signals than copper-line-only DSL signals. Some (or all) connections, shown as antenna beams centered on a twisted pair that represents a wireless signals' wireline-copper link carriage. Figure 1 uses the label "C" for "cell" in various colors for connections that use both wireline and wireless link segments. Figure 1 also shows the wireline connections' subset as accurately "beam steering" the waveforms until the last wireless link in the customer premises (where additional multiple antennas could be used inside the home for further direction of signals to multiple in-home end points, see Section III). Figure 1 shows the end devices as cellphones, but they could be any end devices like computers, tablets, televisions, game consoles, things, etc. As long as the wireline connection supports enough bandwidth for the home, the entire experience appears as if wirelessly connected on the wireless system, a possibly very convenient and efficient form of convergence, at least at the physical layer. For instance, service providers often lament advanced wireless' requisite high capital investment to build more cell sites at a network edge closer to the end users: Deutsche Telekom's CEO in 2018 estimated that such tower construction for the European Union would cost nearly 300 – 500 billion euros [12]. The proposed CSL system reduces such cost wherever use of existing copper is prudent.[6]

Section II begins by describing an infrastructure that uses the existing wires to carry (at low carrier frequency) the cellular baseband signals through base-station-located **intermediate-frequency (IF)** modulator/demodulator converters (the **CSL-IF system**). These CSL-IFs up/down-convert the wireless **baseband unit's (BBU's)** signals to the appropriate carrier frequency for transmission through the wireline connection. Section II builds upon the earlier mentioned work in [1]–[10] with an improved alternative duplexing scheme for the wireline connection's equal downlink/uplink-distortion sharing. This duplexing uses "**frequency-scaled**" wireline-connection characteristics to allow time-division downlink/uplink duplexing while handling Frequency-Division-Duplexed (FDD) cellular systems, and even carrier-sense multiple-access (CSMA). This architecture similarly accommodates Wi-Fi systems, with latency well within accepted standards. This frequency-scaling also allows fair length-independent downlink/uplink sharing of

[5]"DSL" is used broadly to cover systems like ADSL, VDSL, vectored VDSL, G.fast, and G.mgfast in this article.

[6]Even if half the new cell sites could be eliminated, the 300-500B euros of a preceding footnote would be 150-250B euros.

the wireline link's bandwidth, circumventing earlier methods' limitations with link length, crosstalk and spectral-resource placement. Section II also argues that such CSL systems often can perform as well as the best legacy DSL methods in delivering high individual-residence speeds to end devices. The CSL-IF is connected via the wireline connection to the **CSL-RF** that up/down converts and frequency scales **radio-frequency (RF)** signals for transmission through the remaining wireless connection.

Electrical power that the copper may deliver to the home also can optionally energize the CSL-RF. These converters' architecture is simple to avoid expensive home-gateway functionality, otherwise allowing cellular to virtualize its functionality inexpensively within the customer premises. Alternatively, a cellular system's uplink powering through the same copper links is also feasible, see for instance [13], so that a "new-tower" location at the northbound copper interface could be powered if no power were available at that new-tower's location.[7]

Section II specifically suggests how cellular's MCS can be used to implement near-optimal DSL performance with the wireless signals. Section II progresses to consider some essential practicalities like synchronization, device association, and maintenance. The CSL architecture may alternatively place baseband Wi-Fi signals on in-home wireline connections and becomes particularly interesting when viewed with MIMO methods and multipair cabling (as with Ethernet cables) in Section III's YSL (Wi-fi Subscriber Lines). Section IV extends the YSL architecture to with a "massive MAP distributed-antenna system" that improves significantly on existing mesh architectures. In principle, one could envision mixed architectures that use Section II's CSL together with Section III's CSL on multi-pair cabling. For example, one could use CSL on outside-plant cables to bring high-speed wireless connectivity into the building, and then use CSL on Ethernet cables internally to connect to Wi-Fi-capable devices inside the premises. This could be particularly attractive for enterprise deployments, but would also be appropriate for the many homes that today struggle with weak cellular signals and inadequate Wi-Fi coverage. CSL may also simply substitute for "fixed wireless access" by passing the cellular backhaul signals on the twisted-pair connection with termination on a customer-premises gateway.

Section III also investigates MIMO[8] systems, noting that wireless' MU-MIMO signal processing is the same as DSL's earlier successful vectoring. Several different situations that bond multiple wireless/wireline paths become possible in Section III's proposed architectures; these circumvent the creative switching concepts of [6] through exploitation of the current wireless MU-MIMO and/or MIMO capabilities, also introducing a higher-performing CSL-RF+ that uses different (and this article argues optimal) mid-MIMO precoders, as an alternative to those discussed in [10]. Some of these new methods readily allow large performance

[7]Such local powering of large numbers of new cell sites can be a significant contributor to the infrastructure costs.

[8]Multiple Input Multiple Output, see [42].

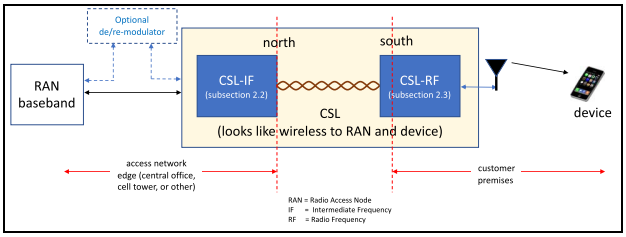

Fig. 2. CSL basic architecture.

increases with respect to existing and contemplated practice. Sections III and IV create a wireless massive MIMO system with coordinated distributed antennas (see [14]) that does not require expensive large (high-power) antenna arrays at every cell tower. The existing wires and existing spectra basically create a bandwidth, and consequent bandwidth efficiency, beyond today's most aggressive cellular and/or Wi-Fi realizations (or predictions). Section V concludes.

II. CSL and Wi-Fi Subscriber Line (YSL) Base Architectures

CSL's initially proposed deployment instance is a simple low-cost/low-power RF conversion at the customer's premises, similarly to previously mentioned innovative work in [1]–[10]. Effectively, this RF conversion completes the radio-access node (RAN) and makes it look effectively as if the entire connection is wireless, albeit actually a cascade of wireline and wireless links. Figure 2's RAN baseband system functionality appears physically at the point where the northbound wireline link terminates (even if that baseband functionality is virtualized in software at another location) via Common Public Radio Interfaces (CPRI) [15] or other X-Haul methods as well described in [16]. A C-RAN system [17] presumably cannot be used because unlike the radio-frequency-over-fiber system option in C-RAN, the copper would not support C-RAN's analog transmission band, and of course the C-RAN's digital options have front-haul data rates that are too high for the copper unless methods like those in [18] become commercially viable beyond experiments in [19]. With CSL, the RAN baseband system is not modified with respect to those in use, the CSL-IF accepts the baseband signals prior to RF conversion and translates them for downlink/uplink transmission on Figure 2's twisted pair. Alternatively, for cases where the RAN baseband is not readily available, Figure 2 also shows the CSL-IF connected (dashed lines) to a downlink demodulator and uplink re-modulator. This dashed-line connection may occur if there is a separate wireless link between the existing cell-tower position and the north end of the twisted-pair cables. Figure 2's CSL-IF modulates/demodulates (downlink/uplink) the baseband RAN signals to/from convenient wireline-compatible frequencies, as Sections II-A and II-B further detail. While Figure 2 shows the CSL-IF conversion at the north wireline edge that connects to Figure 2's RAN baseband, the RAN, including access to the baseband signal, is considered part of the existing infrastructure, while the CSL-IF is new. Figure 2's central shaded box contains CSL's new components; the rest remains the same cellular system without alteration.

A customer-premises-located CSL-RF conversion system completes the up/down carrier modulation at the wireline's south end, effectively implementing a distributed superheterodyne modulator/demodulator across the CSL-IF and CSL-RF systems, conceptually first introduced in [1].

The CSL-RF system may amplify signals but does no digital decoding nor regeneration of wireless signals. Section II-B describes further the CSL-RF system. This article subsequently distinguishes the term **link** from the term **channel.** A **link** will be a physical connection, wireline or wireless, used for communication. A **channel** will be a continuous set of frequencies with a bandwidth that is modulated by a carrier frequency. There thus may be many channels carried on a single link. The channel carrier frequencies (downlink and uplink) are conveyed to the CSL-RF system through a control channel that runs only on the wireline link, which Section II-D further details after this concept's introduction in Sections II-B and II-C. CSL system synchronization will make use of some training signals, the control channel, and a pilot signal as in Section II-D. This use observes and enforces the stringent overall timing advance[9] [20] and IEEE-1588-based [21] synchronization requirements that have not been fully addressed in previous work insofar as distributed antenna systems of any sort may require. Section II-D also describes a wireline channel-sounding procedure that will be necessary to estimate the wireless signal's gross bandwidth that the wireline link can support, as well as to determine the group delay necessary for IEEE 1588 network-clock administration. This method does not rely on embedded signals like previous work, and will have several practical advantages as well as provide more accurate channel and group-delay estimates. The CSL-RF signals propagate wirelessly to and from the end device. Wireline filtering and noise distortion become part of a baseband-equivalent cascaded link, which from a wireless-system perspective appears simply as part of the wireless link. Section II-E analyzes this cascade's performance, particularly estimating any loss with respect to an alternative xDSL DMT system that could fully support maximum data rate on the same twisted-pair channel. CSL uses wireless' inherent bandwidth-adjustment capabilities and MCS methods, rather than attempt various compensation methods in the CSL-RF. Analog amplification that increases equally signal and noise enlarges the entire signal. (Section III will revisit spatial processing at this CSL-RF location.) Section II-F briefly addresses uplink device association to the pertinent cellular system. Section II-G introduces the possibility of remote cloud-based control of the CSL-IF and CSL-RF, which this work suggests may lead to good improvements and yet maintain legacy compatibility.

A. CSL Definitions and Nomenclature

Table I provides CSL's given and derived parameter definitions. The table lists variable names and then

[9]Timing advance here means compensation for the delay of transit that is between the CSL-RF and the location of the baseband signal generation (or regeneration uplink) that would be zero or known well in a system without CSL.

TABLE I
CSL PARAMETERS (BOLD FACE USED IN EXAMPLES WHEN MORE THAN 1 OPTION)

Parameter	description	Cellular Value(s) (CSL) [22]	Wi-Fi Value (YSL)
Given parameters			
Δf	Subcarrier spacing[10]	**15,** 30, 60, 120, 240 … kHz	**312.5** kHz 78.125 kHz
m	expansion factor	1,2,4,8,12,16, 32, 80,160,320	1,2,4,8
N_{FFT}	FFT size	$128m$	$64m$ or $256m$
N_{CE} $\langle N_{CE} \rangle$	Cyclic extension size avg value	$\mathbf{32}m$ or $\left(\frac{1}{7}\cdot 10+\frac{6}{7}\cdot 9\right)m$	$\mathbf{16}m$ or $8m$
$N_{symb/slot}$	Number of symbols / slot (integer)	**6**,7, 12, or 14	10
D	Freq-scale factor	**8/3**	**5/4** TDD 5/2 full duplex
d	Pilot scale factor	1	0.1
$\frac{1}{T_0}$	Master clock	$\mathbf{30.72}m$ MHz	$200m$ MHz
Derived Parameters			
$\frac{1}{T_{slot}} = \frac{\Delta f}{N_{symb/slot}\cdot\left(1+\frac{\langle N_{CE}\rangle}{N_{FFT}}\right)}$	fixed slot clock	2^n kHz *n=**1*** for LTE or *n=0,**1**,2,3…* NR	**25** kHz or 6.25 kHz
$\frac{1}{T} = \frac{N_{symb/slot}}{T_{slot}}$	symbol clock	**12 kHz** or 14 kHz	250 kHz
$\frac{1}{T'} = (N_{FFT} + \langle N_{CE}\rangle)\cdot\frac{1}{T}$	complex sample clock (baseband)	$1.92m$ MHz	$20m$ MHz
$\frac{1}{T''} = \frac{2}{T'}$	Real sample clock (baseband)	$3.84m$ MHz	$40m$ MHz
$p'' \in Z^+$ $p''\cdot T_0 = T''$	Integer divisor of master clock to IF sampling rate	8	5
$\frac{1}{T'''} = \frac{D}{T''}$	DAC/ADC clock	$10.24m$ MHz	$50m$ MHz
p''' *where* $p'''D \in Z^+$ $p'''\cdot T_0 = T'''$	Integer divisor of master clock to ADC/DAC sampling rate	3	4
$f_{IF} = \frac{1}{2T'}$	CSL-IF carrier	$960m$ kHz	$10m$ MHz

[10] All frequencies, including subcarrier spacing, are derived from a master clock as in Table II.

TABLE I
(Continued.) **CSL PARAMETERS (BOLD FACE USED IN EXAMPLES WHEN MORE THAN 1 OPTION)**

Derived Framing parameters (samples per symbol)			
$\langle N'_{samp}\rangle = \frac{T}{T'}$ $N'_{samp} = N_{FFT} + N_{CE} \in Z^+$	avg BB samples/symbol can vary	$160m$ see N_{CP}	$80m$ --
$\langle N''_{samp}\rangle = \frac{T}{T''}$ $N''_{samp}=2N'_{samp}$	avg IF samples/symbol can vary	$320m$	$160m$
$\langle N'''_{samp}\rangle = \frac{T}{T'''}$ $N'''_{samp}=2DN'_{samp}$	avg DAC/ADC samples/symbol can vary	$853\frac{1}{3}m$	$200m$
$N_0=p''' \cdot \langle N'''_{samp}\rangle$	master samples/symbol	$2559m$	$800m$
$N_{silent} = N_0 - \mathrm{p}''' \cdot N''_{samp}$	master samples / fast-silent period	$1599m$	$160m$
$M'_{samp} = \langle N'_{samp}\rangle \cdot N_{symb/slot}$	BB samples/slot	$960m$	$800m$
$M''_{samp} = 2 \cdot M'_{samp}$	IF samples/slot	$1920m$	$1600m$
$M'''_{samp} = D \cdot M''_{samp}$	DAC/ADC samples/slot	$5120m$	$2000m$
$M_0 = p''' \cdot M'''_{samp}$	master samples/slot	$15360m$	$8000m$
$M_{silent} = M_0 - p''' \cdot M''_{samp}$	master samples / slot-silent period	$9600m$	$1600m$

some suggested example values, which Section II-B further describes, appear for both cellular and Wi-Fi transmission formats. Given parameters have fixed value sets, that is they are CSL design inputs. Derived parameters' values depend on the given parameters. When more than one option occurs for a given parameter, this article's examples use the bold-face value.

The given parameters essentially define the CSL system. A slot is the longest time interval T_{slot} of interest and derives from the given sub-carrier frequency spacing and number of symbols per slot. For 3GPP cellular standards/releases in 4G and 5G wireless networks, this slot value often is 500 μs (e.g. LTE), corresponding to a slot rate of 2 kHz that this article's specific cellular example uses; however 1 ms, 250 μs, 125 μs (e.g. New Radio or NR/5G) also find use as per Table I. The example Wi-Fi slot rate is 25 kHz. The integer m is a given integer bandwidth-expansion multiplier. N_{FFT} is a given FFT size used to characterize modern wireless modulators, typically a power of 2; this work considers N_{FFT} given (even though it does depend on m) by a power of 2 multiplier for each of cellular and Wi-Fi. Similarly N_{CP} specifies a cyclic-extension length, typically 25% of the FFT size in wireless, but sometimes 1/2 this value and sometimes averaged over two values as in Table I. The given number of symbols per slot $N_{symb/slot}$ imposes many clock rates used in CSL. D is a frequency-scaling CSL-specific parameter used to ensure time-division duplexing of the same wireline link's downlink/uplink transmissions.

An integer divider of a master clock maintains accurate consistent sample spacing within a burst. The cellular example master clock frequency is $30.72m$ MHz while the Wi-Fi master is $200m$ MHz. When the number of ADC/DAC samples in a slot (or a symbol) is not an integer, there is a residual that is an integer multiple of master clock periods. CSL duplexing "stuffs" these residual master clock periods into the next silent period. The frequency-scaled bursts (time-division bursts), when not in silent period, always have consistent equal spacing between ADC/DAC samples (so the sample clock introduces no distorting jitter). However, when in the silent period, a "stuff" occurs that realigns symbol and slot boundaries. That one "stuff" changes for one sample the inter-sample period spacing, but only on a single zeroed sample that is not used. This "stuff" does not affect the cellular symbol period and sub-carrier spacing (and associated cellular sampling rates), so the cellular system sees a consistent sampling clock. The CSL system also sees a consistent sampling clock on all non-zero burst-mode samples.

Table I's remaining parameters derive from the given parameters as specified in Sections II-B–II-G. YSL throughout will refer to a Wi-Fi example (instead of cellular), where "Y" stands for the "Wi" in "Wi-Fi". The notation $(a)_b \triangleq a$ modulo b or the residual after the largest integer multiple of b has been removed from a. Some of Table I's parameters will become more clear as this article proceeds. Z^+ is the set of positive integers.

This article's use of the term "slot" in the Wi-Fi example is different that the use of the term "slot" that appears in [23].

B. CSL Intermediate Frequency Conversion (CSL-IF)

Figure 3 further details Figure 2's network north edge "radio access node" CSL-RAN component for the index[11] m. This index directly corresponds to intra-band carrier aggregation [24] where contiguous "aggregated" bands simply appear as a wider band. The CSL-RAN could also easily accommodate inter-band expansion by a multiplicative increase of m, typically by the number of equal-bandwidth frequency segments. Figure 3's gray-shaded box shows explicitly the intermediate-frequency (CSL-IF) system. A frequency plan appears below Figure 3's system diagram. The CSL-IF modulates the sampled downlink baseband signal $x_{bb,k}$ by a carrier at frequency f_{IF}. The baseband complex sampling rate is $\frac{1}{T'}$. This multiplication creates a complex analytic signal $x_{A,k}$ at that same sampling rate. The following box interpolates this analytic signal to twice its IF sampling rate $\frac{1}{T''} = \frac{2}{T'}$ and into a real-valued samples by taking the real part after this interpolation. The subsequent buffer box includes any interpolation-implementation delay. Figure 3's heavy red-colored connections are complex signals, while the thinner blue connections are real signals. The real signal then (downlink) passes to the DAC that accepts samples at DAC clock rate $\frac{1}{T'''} = \frac{D}{T''}$. The frequency scaling by factor $D \geq 1$ allows **time-division**

[11] $m \in \{1, 2, 4, 8, 12, 16, 32\}$ in various 3GPP or Wi-Fi standards, but could be envisioned to increase to larger values in OFDM-based millimeter-band use of the future. This article will later introduce difference subscripted-indexed versions of this bandwidth-expansion/scaling parameter for the wireless system, say m_{3GPP} or m_{Wi-Fi} and for the wireline line, say m_{CSL} or m_{YSL} and it will generally be a non-zero positive integer when used. It may also use the notation $m_{downlink}$ or m_{uplink} where the subscript in all cases helps identify the exact use intended.

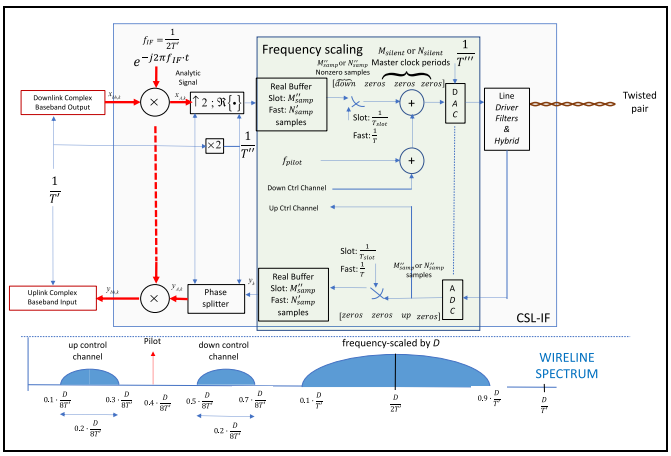

Fig. 3. CSL-IF system (at the access-network edge or AP location with YSL).

duplexing (TDD), and this process is within Figure 3's green-shaded box. TDD sends zero samples between downlink and uplink signal bursts. These zero samples correspond to no transmission, but the CSL-IF and CSL-RF count the number of master-clock periods between the last data symbol's last sample and the next data symbol's first sample (the same counting occurs for uplink). This number of silent-interval clock periods need not be an integer multiple of sampling periods and ensures alignment of Table I's symbol and slot boundaries. With bandwidth expansion, CSL's TDD supports inter-band carrier integration with multiple baseband carriers; CSL's time-division sample bursting into the channel will have successive bursts for each separate discontiguous band, and the analytic-signal construction repeats for each such discontiguous band (Figure 3 only shows this once). Section III-B further describes such bursting for multiple discontiguous streams, which may correspond to different frequency bands and/or spatial streams. The remaining superheterodyne's RF carrier modulation occurs in Figure 4's CSL-RF converter that Section II-C describes. CSL's TDD corresponds only to the wireline link, and thus does introduce new uplink/downlink contention ratios.

Figure 3's complex baseband signal(s) is (are) today[12] present in 3GPP-standards-compliant base stations, taken from a point prior to carrier modulation, in a digital form at the sampling rate. If this signal is not readily available, Figure 2's optional de/re-modulator reconstructs it. Such reconstruction would likely occur if there is a (second) wireless connection between the base station and the CSL-IF. In this wireless extra de/re-mod case only, the possibility of two wireless versions of the same signal in spatial proximity simply creates a multi-path situation that wireless transmission already well addresses. It is possible also that a wire (or fiber) could carry the wireless signals between the base station and the line terminal, either baseband (most likely with a copper connection like another CSL) or as radio-frequency over fiber. These digital time-domain (two-dimensional or complex) samples will recycle each symbol in time index, so for example $x_{bb,k}$ $k = 0, \ldots, (160 \cdot m - 1)$ includes a cyclic extension of $32 \cdot m$ repeated samples $x_{bb,k} = x_{bb,k-128m}$; $k = 128m, \ldots, 160m-1$ for each 3GPP-compliant baseband symbol. This format of extra 25% cyclic extension is sometimes known as the 3GPP lengthened cyclic-extension format.[13] These signals mathematically correspond to Table I's N_{FFT}, Δf-wide tones, where standardized wireless transmission does not excite the upper and lower edge tones.[14] This edge-tone zeroing creates wireless channel frequency guard bands of at least $\frac{1}{10T'}$ above and below the wireless signal, which CSL uses on the low end for pilot and control-channel placement. Figure 1's lengthed-cyclic-extension cellular-example wireless symbol rate is $\frac{1}{T} = 12$kHz, while it is 250kHz for Wi-Fi, as in Table I.

One example-CSL-IF interpolation method repeats the baseband signal's DFT in frequency, but then zeros the upper repeated DFT frequencies and then frequency-translates the remaining signal up through a double-size DFT. This would require a DFT and reverse IDFT to occur in the interpolation function before taking the real part at the new doubled sampling rate. Therefore, it might be simpler if the baseband wireless signal is available already in DFT domain. Any downlink delay in causal interpolation should be reduced from the ensuing time-division buffer's symbol/slot boundary (see Section II-D). Thus, the CSL-IF carrier-multiplied analytic signal will usually leave $\frac{1}{10T'}$ of empty bandwidth from 0 to $\frac{1}{10T'}$ (and a similar amount zeroed at the highest frequencies of the IF output up to $\frac{m}{T'}$). Effectively, the IF modulation re-centers this baseband complex signal to an analytic complex signal centered at f_{IF}, whose real part passes through the channel after undergoing the frequency scaling that the next paragraphs describe.

Figure 3's real buffer time-duplexes downlink and uplink signal samples' entry/exit to the single wireline link. Each baseband "slot" contains $N_{symb/slot}$ successive symbols or $N_{symb/slot} \cdot (N_{FFT} + N_{cp}) \cdot m$ samples in slot period T_{slot} that corresponds to Figure 3's slot clock. These samples convert in succession to analog at the higher sampling rate of $\frac{1}{T'''} = \frac{D}{T''}$. For the cellular case, this usually corresponds to $1/3$ times the master clock frequency of $30.72m$ MHz, so $10.24m$ MHz (as in Table I). The **frequency-scaling** function "bursts" downlink samples into the wireline link and effectively spreads the frequency response downlink (and extracts samples and de-spreads uplink samples). There are two CSL-IF operational modes shown in Figure 3. The "**fast**" mode has the lower additional latency ($<T$) and duplexes by changing direction every symbol. The **slot mode** correspondingly instead adds

[12]Present day "front-haul" or "X-haul" systems impose this baseband-component's availability for instance [16] or [50].

[13]The example's use of 3GPP long-extension format [22] presumes that the wireline link's distortion has longer group delay. The long format has become optional in NR, but for backward compatibility reasons, it is likely implemented mandatorily everywhere. The short-form format has been and could be used also with the consequent derived-parameter changes in Table I. In the fast mode of Section II-C, the length of the cyclic extension becomes indifferent to performance because there are silent-period zero samples used after each symbol for direction reversal, which essentially lengthens the cyclic extension. Wi-Fi also has two cyclic-extension options, and Table I also uses the longer cyclic-extension as the given-parameter example. These silent periods also simplify any necessary clock realignment.

[14]These zeroed edge tones comprise roughly 10% of bandwidth used for Table I's cellular and Wi-Fi examples.

a maximum delay of T_{slot} because it maximally waits an entire slot before reversing direction. The additional slot delay may also be acceptable and depends upon the chosen design parameters; Table I's example-specific delays are considered acceptable, see further Section II-D. These delays will also need incorporation into IEEE 1588 network-timing reference.

The long silent periods offer the opportunity for the CSL-IF downlink (and CSL-RF uplink) to increase the wireline segment's cyclic-extension length, rendering use of short-cyclic-extension-length modes readily feasible. Such an increase can improve wireline-link performance. Any "stuffed" master-clock periods should occur outside such optional cyclic extension but within the silent period. These large zero-sample silent periods can also be used to create a timing advance Δ of the signal that is equal to the negative of the measured group delay (see Section II-D). This advance then will allow any wireless network-timing according to IEEE 1588 [21] to work properly by offsetting the delay between antenna location and baseband-processing site. This is implicit within the CSL system without the need to adjust the exterior system timing. The CSL bursting delay will still be T or T_{slot} but the offset essentially ensures this maximum, and clearly known, delay for network-timing-reference-reporting purposes. The timing-offset generally could be used in many distributed-antenna-system [14] applications with wires and not just CSL, as long as the wireline section between baseband processing and antenna supports the same rough bandwidths as the twisted pair described here (which is highly likely as wires used in distributed antennas are likely to be higher grade than twisted pair). This article later discusses other exploitations of excess zero samples.

The fast-mode zero samples' use also accommodates the short-cyclic-extension mode through allocation of a sufficient number of the silent-period zero samples to a longer cyclic extension (as long as is necessary for best receiver distortion limiting). This tacit extension addresses a concern that some recent 5G 3GPP standards only mandate a short extension that by itself is not sufficiently long for the wireline link. Further TDD-cellular systems have their baseband samples directly input to the CSL-IF and have bursts within those that the CSL-IF can accommodate (for instance in the cellular-example case of $D = 8/3$). Such a TDD baseband signal will have a larger value of m (usually $2m$), but otherwise fits as described above (in terms of m) into the CSL format. In such an interface, the CSL design can usually reduce D because the TDD cellular system is already bursting. Wi-Fi is already TDD (in most uses) and so the Wi-Fi example frequency-scaling increase is consequently smaller at $D = 5/4$; if Wi-Fi were full duplex or used different downlink/uplink frequencies, then $D = 5/2$. This applies for the larger values of m used in millimeter-band cellular systems such as 5G-NR's Frequency Range 2. Thus, CSL works in all the cellular and Wi-Fi frequency ranges with the appropriate value of m.

Cellular wireless' uplink uses "single-carrier" OFDM, which is simply an OFDM-synchronized signal that corresponds to a particular uplink user's few used tones being interpolated via IFFT as a wider "single-carrier," but with effectively the same sampling rate. This uplink signal will aggregate $N_{FFT,uplink}$ uplink tones' input symbols into a single time-division sampled sequence with these $N_{FFT,uplink}$ baseband input uplink symbols in succession, and then add same-OFDM-length cyclic extension to this set of $N_{FFT,uplink}$ signals. This format maintains OFDM symbol boundaries. Symbol-boundary alignment may involve compensation for wireline group delay as mentioned above. This "single-carrier OFDM" purportedly reduces peak-to-average power for uplink transmitters [25] where battery-energy consumption may often be an issue. Because of the constant OFDM structure used in terms of time-division samples, this uplink format does not cause change to the CSL-IF (nor CSL-RF) systems described here.

In the cellular example, Table I's choices allow both fast and slot modes to have the pilot (256 kHz) as a simple integer divisor of an often-used 30.72 MHz master clock (see Section II-D). These choices also place the pilot in one of the safest passbands of a copper twisted-pair channel (see Section II-D). Other pilot-frequency choices and control-channel selections are also possible, but the choices here scale simply with a fixed given symbol rate. Both slot and fast modes also easily allow asymmetry to be proportionately introduced without concern for spectrum planning. For example in cellular examples, this buffering accommodates any asymmetry from 12:0 (broadcast cellular) to 0:12 (all uplink); for instance, 8 symbols downlink for every 4 uplink would provide a 2:1 asymmetry ratio in the format, while 9 symbols downlink for every 3 uplink would be 3:1 asymmetry and 10/2 would allow 5:1 asymmetry. These would be the corresponding ratios of the CSL system's choices of $m_{downlink}/m_{uplink}$. Additional loss of one direction's bandwidth, or use of some excess silent-period samples, accommodates almost any value of $m_{downlink}/m_{uplink}$and thus any asymmetry ratio.

CSL's frequency scaling differs from all previous approaches significantly and allows any wireline filtering distortion to be experienced equally by downlink and uplink signals, regardless of the wireline-copper link's length. Much previous concern for the wireline link's choice of exact uplink/downlink channel consequently abates. Section II-C's CSL-RF removes the downstream frequency scaling, and thus occurs only on the wireline link. A smaller number of samples could be used for direction reversal because wireless transients typically abate in N_{CP} (complex) time samples; however, as in Section II-D, this large number of silent-period samples greatly simplifies timing recovery.[15] The silent period also allows for optional extra services to the customer, even if not needed for extension of cellular's perhaps-too-short-for-wires cyclic-extension enlargement. This new possibility of extra samples' bandwidth re-use also provides considerable opportunity to service providers who

[15]The extra samples might well be exploited for additional non-3GPP signaling or diagnostic purposes as well as for extra training, synchronization, or maintenance signals. Indeed, a separate non-wireless data channel could be inserted for non-3GPP additional service that could be an additional service provided by the CSL system, perhaps for Wi-Fi, Bluetooth or other systems in parallel to the 3GPP system within the home. This would require the presently very simple CSL-RF converter box to be less simple.

may have multiple objectives for their infrastructure build and consequent capital-expense allocation to support various services and applications as per Section II-G. Larger extra-service bandwidths can benefit from a larger choice of D. In effect, the wireless signals' bandwidth for either direction is frequency scaled by oversampling (by the factor D) from its original bandwidth when entering the downlink wire section when that direction is active. The choice of D must ensure that $p''' \in Z^+$. This system remains linear in its baseband-equivalent effect. The channel filtering will be the product of the frequency-scaled wireline-link transform and the following (non-frequency-scaled) wireless-link transform for the overall baseband equivalent channel transfer as in Section II-E (and Figure 9a). This is different than all previous approaches in [1]–[10].

Figure 3's uplink path has similar functionality that corresponds to the reversed direction. Any uplink phase-splitter delay (in causally implementing $y_A(t) = [y(t) + j \cdot \breve{y}(t)|_{t=kT''}]$) is offset from the nominal symbol/slot boundary in the preceding time buffer, where $\breve{y}(t)$ denotes Hilbert Transform. Figure 3 also shows the scaled wireline-only signals' frequency range (downlink and uplink), and then Section II-C's pilot and control channel.

Section III focuses more on Wi-Fi, but one aspect of Wi-Fi that needs attention in this immediate discussion is the contention-based Distributed Coordinated Function (DCF) that may use shorter symbols to eliminate (reduce) contention with multiple users. For example, suppose there is a frame exchange sequence RTS-CTS-DATA-ACK[16] between the AP (Access Point) and STA (station) where the inter-frame space (IFS) between these frames is the SIFS (Short IFS), e.g., of 10-28 μs. The YSL time-duplexed structure then must use the fast mode when the YSL-IF downlink (or corresponding YSL-RF uplink) senses these short symbols; this implies the YSL-IF correspondingly shortens its symbols but otherwise follows the same pattern and relationships in Table I. The corresponding values for the equivalent of N_{FFT} and N_{CP} (the latter of which is often zero in these modes) are smaller than in Table I's Wi-Fi example. This reduces latency to within the limits because the signals can be passed with only 4/5 of a short symbol length extra delay. YSL-IF/RF's also must sense the short symbols when they are present. Also, ADC/DAC & up/down conversion delay will be roughly several samples, so is negligible. Therefore, YSL's additional latency are negligible.

C. CSL-Radio-Frequency Conversion System (CSL-RF) at the Customer Premises

Figure 4 illustrates the customer-premises-located CSL-RF system between the wireline and final south-end wireless links. All ADC and DAC clocks in both the CSL-IF and CSL-RF are synchronized to $\frac{1}{T'''}$, as in Section II-D, and indeed also at symbol and slot boundaries, modulo any timing advances. Downlink CSL-RF silent periods similarly align through the proper number of master-clock periods. Cellular systems and most Wi-Fi also have carriers derived from the same common clock. The slot clock gates the nonzero downlink samples (with distortion introduced by the wireline link) into the buffer. There is additional delay that should be set to equal T (fast mode) or T_{slot} (slot mode) in the CSL-RF for purposes of IEEE 1588 synchronization when/if used. In this way, the reported delay to network timing is then always exactly this symbol period or slot period respectively. During the direction reversal or uplink transmission, the downlink buffer does not fill nor empty. When the downlink is active, the CSL-RF regularly spaces the output non-zero real samples at the IF clock rate and removes the bursting at this IF DAC clock rate while converting these samples into analog for continuous-time modulation to the selected channel carrier-frequency of $f_{c,down} = f_{LTE,down} - f_{IF}$. This operation removes the downlink wireline link's frequency scaling prior to south-bound wireless downlink transmission. The downlink (and uplink) carrier frequencies will be communicated to the CSL-RF system through the control channel. The wireline time-division duplexing will have disappeared at this RF-modulation point, and any frequency-scaled equivalent transfer/filtering of the downlink wireline channel will now be embedded as if it were just another baseband-equivalent wireless link component.

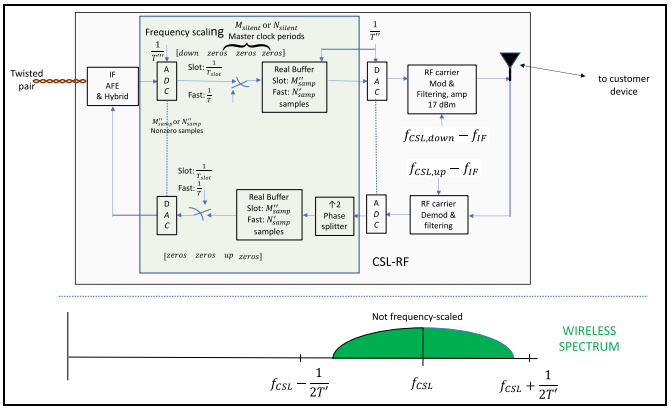

Fig. 4. CSL-RF system at the customers premises (or at extender location for YSL).

Figure 4's uplink path contains the corresponding uplink frequency-scaling functionality that samples the demodulated uplink wireless signal at baseband symbol rate $\frac{1}{T'}$. The CSL-RF interpolates the samples by a factor of 2 to an analytic signal through the phase splitter before buffering for uplink wireline burst transmission during the slot clock's (or symbol clock's) non-zero uplink sample periods. A buffer offset removes any phase-splitter implementation delay relative to the symbol-time start. In effect, this means the phase-splitter function combines with the buffer. Table I specifies the silent period in terms of master clock periods, which is the same as the downlink. Again, the aggregate transfer function will be the product of the frequency-scaled uplink wireline baseband-equivalent transfer function and the baseband equivalent of the carrier-modulated wireless uplink

[16]The Wi-Fi retransmission protocol uses an RTS (request to send), CTS (clear to send), DATA (the actual data sent), and ACK (acknowledgement) sequence to ensure correct transmission and reception, see [23].

TABLE II
CELLULAR-EXAMPLE CSL CLOCK DIVIDERS

Clock	divider p	Variable name	Nominal Frequency
Master Cell Clock	1	T_0	$30.72m$ MHz
Slot clock	$p_{slot} = 15{,}036m$	T_{slot}	2 kHz
Symbol clock (fast slot clock)	$p = 2{,}560m$	T	12 kHz
BB Cellular sample clock	$p' = 16$	T'	$1.92m$ MHz
Analytic Cellular sample clock	$p'' = 8$	T''	$3.84m$ MHz
CSL sample clock	$p''' = 3$	T'''	$10.24m$ MHz
pilot	$p_{pilot} = 120$	T_{pilot}	$256m$ kHz
CSL-IF carrier	$p_{IF} = 32$	T_{IF}	$960m$ kHz
Carrier at a frequency that is an integer multiple n of 2 kHz	$\left(\frac{n}{p_{slot}}\right)$	T_{RF}	$n \cdot (2\text{ kHz})$

(See Section III and Figure 10a). Excess samples again optionally can support extra (non-cellular and/or non-Wi-Fi) services.

D. Control, Synchronization, and Sounding

The CSL-RF system requires initialization, synchronization, and updating. It also needs (in practice) some basic maintenance capabilities for fault location. This subsection addresses these topics. This subsection addresses directly only the cellular-example case. However, the extension to Wi-Fi follows the same steps, just with different absolute clock frequencies.

1) The Pilot: Figure 3's $\frac{D}{20T'}$ pilot continuously transmits downlink during all operation (there is no need for an uplink pilot). As mentioned earlier, this is a very safe[17] placement of the pilot on a twisted-pair link. For the cellular example, this 256 kHz pilot (with $m = 1$) is an integer divisor of the cellular master clock running at $1/T_0 = 30.72$ MHz (or optionally $1/T_0 = 245.76$ MHz for wider bandwidths, or even just optionally $\frac{k}{T_0} = 30.72k$ Mhz, where k is a positive integer, for exceptionally wideband systems if needed). Phase-lock loops drive the CSL-IF and CSL-RF master clock so that the derived pilot has low/zero phase error. This CSL pilot has 128 cycles per 2-kHz slot-clock period T_{slot}. The cycles have upward zero-crossing aligned with the start of each 500 μs slot-clock period. All necessary clocks will be integer divisors of the master clock, except for the carriers that are rational-fraction multiples of the master clock.

Table II illustrates the various relationships for the cellular example. The IF carrier frequency as well as the RF carrier frequency phase lock at rational-fraction multiples of this pilot, or at integer multiples of the slot clock (as required by 3GPP[18])

[17]Safe here means that the transfer band on the wireline link has very low attenuation so the pilot will pass.

[18]These all can also be GPS synchronized between 3GPP RANs by standard with accuracies specified in the IEEE 1588 standard, which instead works with a network clock.

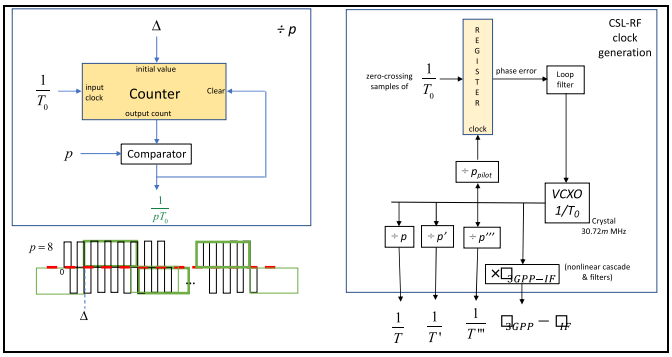

Fig. 5. **Architecture for CSL (CSL-RF) general clock synchronization.** (the symbol x means frequency multiply, which is achieved with nonlinear elements and filters).

by phase-locking to a voltage-controlled crystal oscillator (VCXO) at the master-clock frequency. The CSL-RF system also generates $\frac{1}{T'''}$ and the carrier frequency. For wider bandwidth cellular, the easiest clocking solution likely scales the VCXO crystal to a multiple of the master clock frequency with $m = 320$ for the widest cellular bandwidth of 400 MHz (which is unlikely to be used on wireline links), which would require a crystal at 9.8304 GHz. It is presumed that the CSL-IF and CSL-RF are designed with view of the specific range of cellular equipment types that they are intended to support. More reasonable intermediate bandwidths could use 3GPP's higher master clock of 245.76 MHz (which serves up to $m = 8$ or 10-MHz-wide cellular channels). With the CSL-IF's frequency scaling, a 10 MHz cellular channel will consume 26.7 MHz of wireline-link bandwidth with time-duplexing enabled (keep in mind all DSL systems also lose bandwidth for duplexing that exceeds a factor of 2 for symmetric transmission). Such 26.7 MHz of useful bandwidth might well be representative of wireline-link lengths less than or equal to 1 km. Shorter lengths would encourage higher frequency local VCXO-based crystals in the CSL-RF, which would still be driven by the phase error measured at the nominal pilot's zero crossings (that is divided by a counter with value p_{pilot} from the master clock). At the $10.24m$ MHz CSL ADC/DAC sampling rate, these $0.256m$ MHz zero-crossing samples occur every 40 (or really 20 samples if phase locking uses both the pilot's positive and negative slope crossings with simple alternating sign) sample periods. Sophisticated phase-error interpolation could use all pilot samples, implemented possibly in the loop filter. Figure 5 illustrates all clocks' generation from the pilot. For more information on various cellular clocking and carrier phase-locking and regeneration, see [20]. Table I shows that all clocks have a common generation, and more importantly implies positive-slope zero crossings aligned with the slowest slot clock's positive-slope zero crossing. As always, the high-frequency carriers require synthesis from the master with local nonlinear frequency-multiplication circuitry, now at the CSL-RF, as in Figure 5. Figure 5's offset Δ is the negative of the group delay in master-clock periods, as discussed further here in Section II-D. The preceding CSL-IF-downlink and CSL-RF-uplink buffers delete Δ.

The PLL must phase-lock to within 1 μs accuracy of cellular's symbol clock. The CSL pilot will have at least 40 dB SNR on any usable wireline link. Fixed-line noise generates phase jitter. The wireline segment has no other jitter source because there is no Doppler nor carrier offset[19]. This 40 dB corresponds to a 20 ns phase-jitter standard deviation[20] at 512 kHz (512 kHz is double the pilot's 256 kHz, but both pilot zero crossings can be used for phase-error generation with alternating sign applied). The example's symbol clock is 12 kHz and the fixed-line jitter offset of 20ns is well below the cellular's 1 μs requirement. Thus, the pilot itself readily maintains the clock accuracy for the symbol synchronization (as long as the system estimates group delay and offset so that the IEEE 1588 reported delay is a symbol or slot period correctly, as in Section II-D3). However, the carrier-offset requirement is more stringent. 3GPP standards require recovery from Doppler shifts corresponding to a vehicle speed of up to 200 km/hour. At 60 GHz carrier, this is roughly 10 kHz, and thus 1 kHz at 6 GHz, 100 Hz at 600 MHz. 10 kHz corresponds to a period of 100 μs. The carrier-to-pilot-frequency ratio is roughly 120,000 (60 GHz / 500 kHz), which means that the pilot's jitter standard deviation needs to be about 0.50 ns, or a factor of roughly 40 below the pilot jitter. This implies averaging of $40^2 = 1600$ phase-error samples. Fortunately, with 512,000 pilot zero crossings per second, the PLL loop bandwidth need only be about 320 Hz (so 3 ms recovery/training times for the PLL), which is well within a wireline link's coherence time (at fastest, several seconds) [26]. So, the simple pilot system will have any frequency-offset/jitter dominated by cellular's wireless-link jitter and frequency offset (perhaps not surprisingly, but roughly stated and assured here anyway), which the cellular design and specifications already accommodate.

2) Channel Sounding and Group-Delay Offset Estimation: 3GPP cellular standards require roughly 1 μs symbol-boundary accuracy across all adjacent base stations. This requires a common clock source (sometimes a GPS clock, or more often a common network clock) and accurate delay measurement from that clock source to the wireless transmission point through IEEE 1588 protocols. The CSL-RF will add T or T_{slot} to this and report through IEEE 1588. Since the CSL-RF moves the antenna point relative to the cellular base station, the CSL systems must accurately estimate the group delay through the wireline link and then offset it in buffers to ensure the reported delay IEEE 1588 is correct. Typically, the cellular system itself has an ability to handle differential delays between the network clock and various physically distinct antenna locations. However, this IEEE-1588-based system [21] will not accommodate wireline-link delays automatically. Sometimes field-installation technicians will know the wire's length and manually adjust the offset for 1588 on installation. However, the CSL system will inherently offset this delay by effectively deleting samples from the preceding silent period to make it appear as if the signal were advanced by the negative of the group delay. Thus, the reported is one symbol period (fast mode) or one slot period (slot mode), thus this reported delay is a constant not dependent on measurements. Similarly, the upstream signal can be advanced by using also the silent periods' extra samples. The silent periods' large number of extra samples maintain both directions' frame boundaries, following 3GPP's use of a timing advance for the same purpose [20]. The constant-delay maintenance essentially occurs in the buffers of the CSL-IF downlink and CSL-RF uplink. This subsection describes the CSL system's estimation of this group delay. This process also finds general use in cellular systems that employ distributed/coordinated antennas, where each link maintains delay from a common network clock source.

CSL wireline link's time-division use permits round-trip delay measurement from the CSL-IF downlink input to the CSL-RF and back to the CSL-IF uplink output (the one-directional delay then divides this estimate by 2). The methods here follow the basics described in [26]. Such a measurement is feasible in the proposed method's wireline link through what is known as **loop back**. Figure 4's green shaded box connects the downlink and uplink signals before the final downlink DAC and after the uplink ADC during loop back (small downlink/uplink delay asymmetry will be handled by the buffer index Δ on the count-downs of Figure 5's master clock). The CSL-RF will perform loop back (thus cellular signals do not pass during loop back) and transmits a known symbol L_0 times. Loop back is not feasible in any of the earlier systems proposed in [1]–[10]. A recommended loop-back symbol would be the chirp signal $X^0_{bb,n} = \frac{1}{\sqrt{128m}} \cdot e^{j\frac{2\pi}{128m}n(n-1)}$, with n as the frequency/tone index, but with zeroed channel-edge tones. This signal has constant amplitude and known phase on used tones. It can be precomputed and stored for use in sounding (probably stored in the time domain after inverse transformation and cyclic extension). Other signals are possible. This signal uses the same cyclic extension as cellular. This chirp signal's loop back occurs after synchronization to the 256 kHz pilot. (Continued phase lock is possible by sending the pilot continuously during loop back. Simple measurement of the pilot delay, however, is not sufficient because it is not in the CSL signal's pass band, but $X^0_{bb,n}$ is in that passband.) The controller-stored signal returns to the uplink cellular interface where the CSL-IF will capture and store it; then the CSL controller likely computes DFTs (which need not be real-time) of that stored signal. The controller divides the DFT output for each used frequency by the known DFT value for the fixed training (chirp) sequence. The controller calculations then average this channel-transfer estimate over all L_0 symbols. A good estimate has

$$\lim_{L_0\to\infty} \mathrm{E}[\hat{H}_n] = H_n \quad \text{and} \quad \lim_{L_0\to\infty} var\left[\hat{H}_n\right] = 0 \tag{1}$$

The channel output for tone n of training symbol l is

$$Y_{n,l} = H_n \cdot X^0_{bb,n} + N_{n,l} \quad \forall \quad l = 1, \ldots, L_0. \tag{2}$$

The control processing estimates channel gains H_n by (the inverse need not be stored when the sounding signal has

[19]There is no carrier offset because all the symbol, sampling, and carrier clocks for the CSL segment all derive from the same source clock.

[20]512 kHz has a period of 1.95 μs (or roughly 2.0 μs), and since e^x for small x is roughly $1 + x$, then 40 dB corresponds to a factor of 100 and thus 20 ns.

constant and thus known amplitude):

$$\hat{H}_n = \frac{1}{L_0} \cdot \sum_{l=1}^{L_0} \frac{Y_{n,l}}{X^0_{bb,n}} = H_n + \frac{1}{L_0} \cdot \sum_{l=1}^{L_0} \frac{N_{n,l}}{\left|X^0_{bb,n}\right| \cdot e^{j\theta^0_n}}, \quad (3)$$

where $X^0_{bb,n} = \left|X^0_{bb,n}\right| \cdot e^{j\theta^0_n}$. This estimate's expected value equals the channel because the noise is zero mean, so

$$E\left[\hat{H}_n\right] = H_n, \quad (4)$$

an unbiased estimate. The estimate's variance follows from the noise energy per (complex) dimension σ_n^2 as

$$var\left(\hat{H}_n\right) = \frac{1}{L_0} \cdot \sigma_n^2. \quad (5)$$

Thus, the channel-gain estimate improves linearly with the number of repeated training signals. This accuracy will already be very good for most diagnostic purposes with $L_0 = 10$-20 symbols. For delay estimation, the phase is more interesting. Presuming such large values of L_0, the ratio becomes

$$\arg\left(\frac{H_n}{\hat{H}_n}\right) = \left(\theta_n - \hat{\theta}_n\right) = \delta, \quad (6)$$

where δ is a small phase error in the estimate (Equation (6) drops the tone index n, presuming this error is small and essentially random over all the tones). Using the approximation $e^x \cong 1 + x$ for small x, the phase-error variance, or the jitter, also decays linearly with the training period (once converged for amplitude). This means the phase-jitter standard deviation decays with the square root of the number of training samples.

The phase over the used tones can be subtracted from adjacent tones, and the slope estimated. That is

$$\text{delay} = -\text{slope} \cong \frac{1}{\bar{N}} \sum\nolimits_{n=N_1}^{\bar{N}+N_1-1} \frac{\hat{\theta}_{n+1} - \hat{\theta}_n}{2\pi\,(15kHz)}, \quad (7)$$

where $\bar{N}$ is the number of non-zero-energy tones, and N_1 is the first index in the non-zero set. The phase-noise estimate's variance in the numerator of (7) is double the jitter estimate, but otherwise the variance in this slope estimate also decays linearly with the square-root of the number of training symbols and used tones. A 12 kHz symbol clock has a period of roughly 86 μs. This needs to be reduced by a factor of 100 to meet the 1 μs 3GPP specification. This means (since $\bar{N} \geq 100$ because most systems use this many tones) that $L_0 = 100$ will suffice. This is a loop bandwidth of 120 Hz, well in excess of wireline temperature-induced phase changes (few Hz). The CSL controller can occasionally update the group delay by inserting the chirp signal in the silent period's middle samples. In fast mode, this controller can insert a shorter symbol of length $64m + 16m = 80m$ in the middle of the extra zero periods to update channel estimates. This need not occur on every slot (1/10 of the slots would readily suffice).

This measured group delay is the round-trip group delay, and thus doubles the estimated value because the signal traverses the link twice, once in each direction. The CSL-RF control processor can also apply Equation (3) to the chirp training signal before loop back. This then directly estimates the downlink group-delay. The uplink group-delay estimate will be the difference. Implementation differences may cause these two downlink and uplink delays to be unequal, so this method improves upon simple divide by 2. The CSL-RF communicates its downlink group delay over the control channel to the CSL-IF, which then computes the difference, relative to half the RAN's IEEE-1588-reported round-trip delay when such adjustment is necessary. This should be computed in samples of the master clock period T_0. If the downlink group delay estimate is longer than the half-round-trip delay, this buffer control subtracts this amount from the Δ value for the T''' counter (modulo p'''); correspondingly, if the delay is shorter, the controller adds this amount to Δ. This process fine tunes the CSL-RF's symbol emission times to be well aligned with other 3GPP cellular RAN's emissions.

TABLE III
3GPP CHANNEL BANDWIDTH'S CORRESPONDING WIRELINE LENGTHS

3GPP Channelization (MHz)	Scaled Bandwidth	Max twisted-pair length
1 (or 1.4 exactly)	500 kHz – 5 MHz	2 km
3	500 kHz – 12 MHz	1.5 km
5	500 kHz – 25 MHz	1 km
10	500 kHz – 50 MHz	500 meters
20	500 kHz – 125 MHz	200 meters
100	500 kHz – 625 MHz	100 meters
200	500 kHz – 1250 MHz	50 meters
400	500 kHz – 2500 MHz	20 meters

A wireline link of less than 2 km will generally support at least 3GPP cellular's lowest channelization, whose frequency scales to 5 MHz. Shorter lengths will support wider 3GPP cellular channelization up to 100 MHz.[21] Table III illustrates the match of 3GPP channelization to twisted pair lengths and the suggested rough transmission band. Table II presumes that all crosstalking systems in the same twisted-pair binder use the same CSL system. The need for legacy xDSL spectral compatibility is negligible in systems that transition to CSL upon deployment of a new cell within a neighborhood. However, as in Section II-F, it is possible to burst-mode

[21]Coaxial cable can support 5G's widest bandwidth 200 (1250 scaled) MHz and 400 (2500 scaled) MHz channels (if unoccupied by other cable modem signals), but longer twisted pairs can experience severe attenuation above 1 GHz.

align CSL transmissions with G.fast's directional TDD bursts, albeit adding some degree of buffering complexity, particularly taking advantage of the many zero samples associated with frequency-scaling. A VDSL spectrum mask could be applied to the CSL-IF downlink and CSL-RF uplink transmissions to reduce crosstalk, and this would appear to cellular as severe spectral fading, necessitating an MCS selection with heavy redundancy in code and small constellation size.

The cellular base station (or the Wi-Fi AP for YSL) must know the possible channelization, and the CSL-IF must know the carrier frequency, or, equivalently, what is the maximum value of m that can be used. The same channel-estimation process will also provide an indication of channel gain/attenuation across the band of the $X^0_{bb,n}$. Channel sounding determines the maximum possible usable bandwidth by attempting successive values of m or through direction inspection of the channel-transfer magnitudes. The CSL-RF control processor best computes m from the downlink sounding sequence $X^0_{bb,n}$. Such CSL-RF-located measurements (by an identical process to the CSL-IF described above) thereby provide the wireline link's channel transfer function. For a simple rule, the cellular-receiver designer (who will know their own error-decoding/erasure algorithms) would in even reasonable unsophisticated designs allow for recovery of at least 25% of the Coded-OFDM tones with at least one of the allowed MCS options (see [27] for code erasure and recovery basics and that MCS allow rates of 1/2 and 3/4). Thus, this simple rule would lead to a CSL-IF rule that any band corresponding to a value of m that has more than 25% of its active tones reporting an energy level below -100 dBm/Hz should not be used. The -100 dBm/Hz corresponds to a level at which the wireline link would have an SNR that may begin to limit performance (even though such a signal and the associated wireline noise would be amplified before transmission from the CSL-RF).

3) Maintenance, and the Control Channel: Figure 3 suggests a minimal control channel using simple modulation (BPSK with redundancy) below 500 kHz. Data rates of 100 or more kbps are readily feasible with high reliability to pass control information to/from the CSL-IF and CSL-RF. Further redundancy and acknowledgement with repetition might also be considered on critical commands. The control channel has some basic functions:

1. place the converter in sounding mode;
2. set the uplink and downlink carrier frequency values for the converter to wireless interface;
3. initialization; and
4. various maintenance/diagnostic functions for the line channel.

Control channel signals can also be used to facilitate cloud management, as in Section II-G.

A control channel uses a simple bit-level protocol like HDLC [28] carried by the BSPK stream (presumably using QPSK with rate 1/2 code for protection). The CSL-IF/RF manufacturer can define simple control commands for the items above. HDLC allows definition of carried parameters, queries, responses to queries, and data in a low-cost manner. Other protocols could also be used.

E. Performance of the CSL Wireline Link

The MCS or "loading" methods [29], used in 3GPP Cellular, Wi-Fi, and DSL respectively, are similar and offer an ability to adapt data rate and coding parameters to the severity of channel distortion. For instance, cellular's resource allocation [30] has a resolution of 12-tone resource blocks that are each 180 kHz wide. These blocks also typically span 1 *ms* time interval or equivalently 12-14 successive symbols[22] in the cellular-example case. Such cellular resource blocks can be energized (carry data) or are not used (zeroed in energy). The resource blocks are successive in frequency over a cellular system's channel range. By comparison, G.fast systems today use 51.75-kHz-wide tones, or resource blocks, that also can be selectively energized or zeroed. G.mgfast systems have an option to use instead 207-kHz-wide tones, so G.mgfast has less frequency resolution than cellular's 180 kHz. The loading system for G.fast allows constellations from 4 QAM to 4096 QAM, while 3GPP Cellular allows 4QAM to 1024 QAM, almost the same (although only for even-integer numbers of bits/tone) within each resource block, but the authors anticipate that future 3GP Cellular standards will increase this to 4096 QAM. Reference [29] shows there is a theoretical equivalence, however, if the codes used are sufficiently powerful, just with different options selected for cellular's Coded Orthogonal Frequency Division Modulation (C-OFDM) or for DSL's Discrete MultiTone (DMT) ***as long as both use exactly the same power spectral density***. Cellular's bit-interleaved punctured convolutional (or LDPC) options are sufficiently flexible to allow the same coding power as G.fast's interleaved combination of 16-state four-dimensional trellis codes with outer Reed Solomon. Wi-Fi resource blocks in recent standards have MCS, but the frequency resolution is 20 MHz, so the same resolution as DSL and/or cellular is not possible in YSL. Nonetheless, situations in which Wi-Fi might be used will have much shorter length copper twisted pairs, and thus performance loss caused by lack of resolution may be acceptable.

An important concept in physical-layer transmission on any medium is the relationship of achievable **data rate** b in bits per complex dimension with **signal-to-noise ratio**[23] (SNR)

$$b = log_2\left(1 + SNR/\Gamma\right). \tag{8}$$

Forney introduced ([31], Chapter 1) the gap parameter $\Gamma \geq 1$ for practical systems to reduce achievable data rate by an amount that is independent of this data rate b and a function only of the code used and the target error probability. There is an achievable data rate that applies to the connection's copper section b_{Cu}, and the total access data rate b can never exceed this data rate so $b \leq b_{Cu}$ even if a digital regenerative repeater were to be used in the home gateway. Equivalently,

$$SNR \leq SNR_{Cu}, \tag{9}$$

[22]A variable-length cyclic extension is used on symbols within the slot to ensure $1920m$ samples in each 1 ms slot.

[23]The SNR is the ratio at the channel output's corresponding dimension of signal average sample energy to the noise average sample energy. This formula is for an additive white-Gaussian noise channel (AWGN) that commonly models wireline and wireless channels.

and therefore any supposition that an intermediate regenerative relay that could be placed at the south end of the twisted pair (e.g., a femtocell) would help increase fundamental data rate is false,[24] if the wireless path's maximum data rate is already limiting. In effect, there is no data-rate loss in simply sending the wireless cellular signal through the entire wireline/wireless cascade to the end device (a more general theory of such relay bounds can be found in the work of El Gamal, Mohseni, and Zahedi [32]). There is value in amplifying that signal (-and-noise sum) to reduce further wireless-link-noise-induced rate loss in the wireless segment beyond the copper segment,[25] but this does not increase the access network's end-to-end data rate if (9) still holds.[26] (Clearly with higher-bandwidth fiber's use, the number of feasible transmission dimensions might be higher, but the same principle applies – the data rate cannot exceed the lowest data rate of a series of connection links. Likely fiber's larger number of feasible dimensions would leave the wireless link limiting the cascade.) Thus, Figure 4's simple up/down CSL conversion of cellular signals fundamentally loses nothing with respect to a femtocell that might otherwise have been attached to the same wireline link.[27] Duplexing (whether time or frequency) must be used in all normal DSLs and also CSL (when there is just one wireline link, see Section III), and this work presumes the various methods have comparable losses. Consequently, the remaining significant performance limitation in multicarrier transmissions, like those used in cellular, DSL, and Wi-Fi, is the frequency resolution. Frequency resolution is the bandwidth of the narrowest transmissions that must all carry the same energy/dimension. If one system is closer to the optimum (Shannon water-fill) power spectral density than another, that system will perform better if the applied codes above modulation layer are roughly equivalent (that is both codes are pretty well selected, as is the case in modern systems). CSL's wireline-link frequency scaling increases cellular's 180 kHz resolution to 480 kHz. Cellular systems allocate one or more resource blocks to a user depending on that user's need for data rate. Clearly, G.fast and even G.mgfast have better resolution than the frequency-scaled CSL system, by either a factor of about 2.5 (G.mgfast) or 10 (G.fast). A worst case for any rapidly decaying edge in CSL cellular's wireline link would be about half of the equivalent bandwidth should have been zeroed and the other half used. A severe worst-case assumption might be that this at most happens at most 2 times in any given channel, meaning that there are 500 kHz of bandwidth that was incorrectly excited with respect to optimum. For a system with the minimum bandwidth of say 2 MHz tones (leaving pilots and edge tones out of the 128 minimum), this represents a 25% loss in energy (-1.3 dB). Further, to recover the data sent on the 25% of tones (that would be lost or at very high probability of error) requires a code with that amount (and at least decoder erasures or more sophisticated iterative decoding presumed) in redundancy or 25% (or at least 25% of the codeword must be parity/redundant[28]). Effectively the 1.3 dB energy loss and the total rate-loss equivalent in dB is

$$-1.3 + 10 \cdot \log_{10}\left(\frac{2^{.75 \cdot b} - 1}{2^b - 1}\right) \text{ dB}. \tag{10}$$

This loss is about 3.5 dB for simple BPSK (so $b = 1$) and increases to 10.3 dB for 4096 QAM (or $b = 12$). The loss is greatest for narrow channels, but if the FFT size increases to 1024 (so that the channel bandwidth is closer to 20MHz, then this loss reduces to 5% errored bandwidth ($-.23$ dB) and 0.95%, or equivalently to an additional 0.3 dB, so .5 dB total loss for BPSK and about 3 dB total loss for 4096 QAM, see [29]. For wireless transmission, the error probability relationship to SNR loss is less strong (because of random fading on the wireless link) and these worst-case loss levels appear within an acceptable range. DSL systems use today at least a 6 dB margin to guard against time-varying noise on the wireline link. This time-varying noise is equivalent (through an equivalent channel model, see [31], Chapter 7) to a time-varying channel gain in wireless. Wireless channels may allow for log-normal fading (although in the case described here, the wireless link with log-normal fading will be shorter) with a standard deviation of 6-8 dB on a full-length wireless channel, and perhaps less than 6 dB on the shorter wireless in-home link segment, especially with some power control. Cellular's codes already accommodate such variation. So the cellular system's slightly better codes and reduced margin help it to offset any DSL-higher-resolution performance improvements. Thus, the CSL system might even perform better on the wireline link than the DSL system would have (basically, wireless uses more robust codes for time-variation, making the "margin" unnecessary or at least allowing for its significant reduction). DSL systems do use physical-layer retransmission protocols (see G.inp [33]), but cellular's more advanced Hybrid ARQ (a good tutorial on this subject appears in [34]) does not have an exact equivalent in DSL. DSL's retransmission methods might thus be argued to allow some reduction in applied margin, but field practice and standards do not allow margins less than 6 dB in the authors' experience.

[24]This statement should not be confused as contradicting a more general theory of repeaters. This simply notes that the given twisted pair saves some spectrum and has a maximum possible data rate (or capacity) that will be a limit on the cascaded link's data rate. If placement of repeaters anywhere is allowed, that represents a different situation, see [32].

[25]Such amplification would return total emitted power in the home to roughly 17 dBm, the signal power often used by for instance Wi-Fi in the home. However, SNR would not improve.

[26]Clearly if a higher-bandwidth fiber is used, then the number of dimensions feasible for transmission might be higher, but the same principle applies – the data rate cannot exceed the lowest data rate of a series of connection links. Likely fiber's larger number of feasible dimensions would leave the wireless link limiting.

[27]The femtocell presumably also having a much higher cost and complexity, not to mention issues of crosstalk between such femtocells and with the base cell.

[28]For instance, cyclic codes like Reed Solomon codes are known to be able to correct up to the number of parity symbols in a codeword if the erasure locations are known. Thus, if there are 4 erasure locations (unreliable positions detected by the receiver signal processing and demodulation process), they can be marked as erasures and corrected. This is essentially a best case on use of redundancy. Most wireless 3GPP/Wi-Fi systems should be able very reliably to detect erasure locations in the OFDM demodulators uses simply by looking at the individual tones' signal strengths relative to expectation, see for instance [27] on cyclic codes.

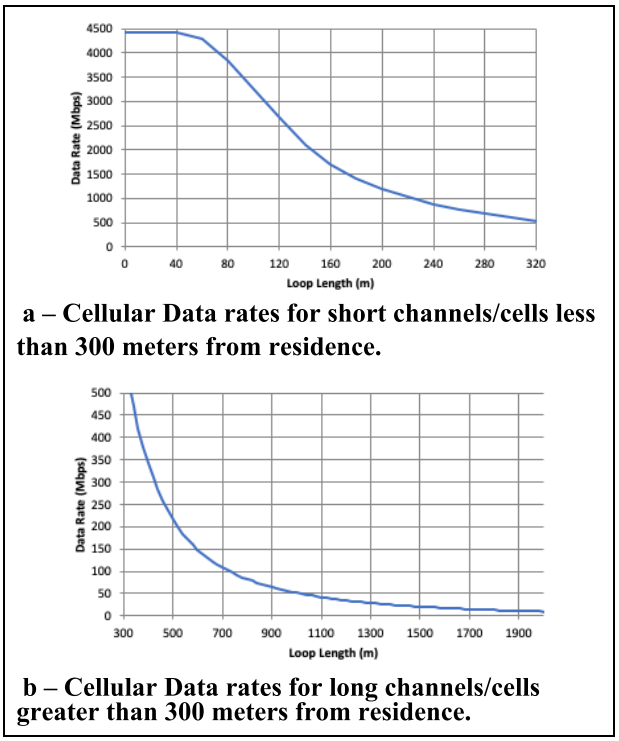

Fig. 6. (a) Cellular Data rates for short channels/cells less than 300 meters from residence. (b) Cellular Data rates for long channels/cells greater than 300 meters from residence.

Comparisons here assume that link and higher-layer protocol losses are otherwise roughly equivalent in today's cellular and DSL systems (both having throughputs well below actual bit rates on the connections) because of these overheads. For methods that allow detailed analyses of these systems and verification of the wireline approximations, see [35], Chapter 3, as well as [36]. Thus, cellular's resolution loss with respect to optimized DSLs is at worst-case a few dB. This may be a small price to pay for the flexibility and cost savings that a CSL system would bring to deployment costs, operation costs, and facility of converged network use.

Figures 6a and 6b illustrate the estimated total data rate (upstream plus downstream) calculated with a 180 kHz resolution versus line length. The total also includes extra data channels that would maximally use the silent periods.

F. Uplink Association

A cellular client device, sometimes called a "UE" for user equipment, nominally searches certain frequency bands, and then searches for channels within those bands for downlink signals. A similar search occurs in Wi-Fi, albeit simpler over a smaller number of bands. The cellular UE has a service provider's SIM card that typically prioritizes certain bands (presumably those of the service provider and any roaming partners) for the channel search.[29] In the CSL case, the CSL-RF downlink carrier frequency presumably is in those searched bands, which carrier frequency is communicated to

[29]Some modern smartphones instead have SIM-independent searches that use the device's geographical location.

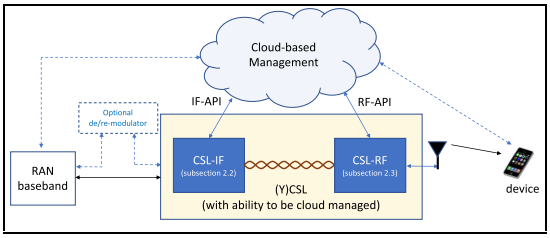

Fig. 7. Cloud-managed CSL (or YSL-Ethernet, see Section IV).

the CSL-RF through the CSL control channel. The cellular downlink signal (once found by the client device and after initial synchronization) will be decoded for a fixed/known-code Physical Broadcast Channel (PBCH) that has (at 40 ms intervals) embedded control information intended for UE's. That information will provide the uplink carrier frequency that is associated with the downlink and upon which the UE uplink signals can transmit (and thus associate to cellular and the uplink carrier frequency used by the CSL-RF, which also knows that carrier through direct supply or by itself decoding the PBCH while it passes). Multiple UE's may use the same downlink with different resource blocks. The same number of corresponding UE's that the cellular system can handle without CSL remains the same with CSL. Similarly, the cellular uplink system will assign different resource blocks to be transmitted on the same uplink carrier by the different UE's (3GPP Cellular has an uplink random-access channel, RACH, that can be used to address multiple UE's who initially try to associate at the same time). This process, other than carrier frequency to use, is transparent to the CSL system. Section III addresses situations with multiple aggregated interband carriers.

For many reasons beyond transmission (like security), the client device should associate with a specific RAN, similar to what is done with 3GPP Cellular's association without CSL, Bluetooth pairing, or Wi-Fi SSID selection today. This presumably continues present practice with CSL again being transparent also to these security issues. Once the association occurs on a common known frequency, information to initialize at other specified known carrier frequencies is possible thereafter. Thus, the client device need not know it is talking to a CSL or directly to a base station. The CSL systems simply need to know the carrier frequency desired by the cellular service provider.

G. Cloud Control of the CSL-IF and CSL-RF, and the Extra Channel

CSL and/or YSL cloud management appears in Figure 7. [37] and the many references therein investigate such cloud management. The cloud controller has access (through an application-programming interface or API) to the CSL-IF and CSL-RF. Probing functions collect various maintenance data (such as that in Section II-D) within these two systems. Such probing can for instance use Section II-D's channel sounding. Only one of the (Y)CSL-IF and (Y)CSL-RF needs an external cloud connection and the other consequently and indirectly also connects through the control channel.

This cloud interconnection can be a low-speed cellular-user channel for an IP address assigned by cellular to the CSL-IF, which the CSL-IF's control processor (in full software only) implements. This cloud-API channel is thus a low-bandwidth "internet of things" connection, thus treating the CSL-IF's cloud control port as one of those "things." A more efficient method might use the CSL's silent time periods for a wireline data connection to customer premises' CSL-RF. Then any non-cellular (legacy or otherwise) home-application devices could continue service in the absence of cellular activity; for instance, an existing home Wi-Fi connectivity might consist of only non-cellular devices that require service. Such existing services would otherwise have been supported by a fixed-line capability on the twisted pair. For instance, DSL's medium-access-layer protocol could support a data stream (downstream and upstream) at the line terminal (north side), and now CSL replaces that system. That existing connection's support could add the IP address for the CSL system (the (Y)CSL-IF and/or the (Y)CSL-RF). An IEEE 1905 protocol [38] could be used to encapsulate the existing internet connection signals at the north end and now send them over the **extra channel** created by use of (otherwise) silent periods. The control channel itself also has available bandwidth for such service even when downlink and uplink signals are present. The bursts would allow a modulation system of the designer's choice, and the cellular and Wi-Fi examples have respectively $200m$ samples/symbol in CSL and $80m$ (full duplex) and $40m$ (half duplex) samples/symbol in YSL that are available for such legacy use. These would for example support easily data rates of a few Mbps (a CSL-IF to CSL-RF bursted DSL system in effect then exists that replaces an existing one at about 1/3 the existing one's data rate at the sampling level, but with the remaining 2/3 being used by cellular). This system could multiplex the DSL processor output samples of an existing ADSL modulator within the bursts fairly easily (and the DSP needs for such designs would be only a small computational increase for the local processor, especially running at lower speeds (apart from the higher-speed sampling rates in the bursts) to decode the lower data rate. Such systems do not need a full cellular baseband demodulator to capture cloud control signals sent to them. Such systems would service existing legacy services and the cloud-control communication. The CSL-RF could interface to a fixed-wireless-access gateway's northbound side to implement in-home distribution (although this has the price of an entire gateway).

The (Y)CSL-RF can measure uplink wireless power levels (and can infer them downstream, or even intercept them for certain management packets that pass through the connection). The CSL-RF can also control power levels and could adjust certain channels' carrier frequencies to appear contiguous at the AP when indeed they are discontiguous on the actual channel. In effect, a more flexible system is created through the cloud management, allowing various multi-user methodologies or resource management to be used (for instance the ESM methods in [37]). Section III discusses this further. A wireline link that is an Ethernet cable of 4 pairs (8 wires) creates a wide variety of possibilities, which Section IV further discusses, to create a very efficient YSL-Ethernet-based system. Figure 4 shows optional dashed-line connections to the device and to the RAN, which could allow additional system options in the system that are particularly synergistic with opportunities created by RAN virtualization or applications/services' control. This article does not further investigate cloud management, other than to say it can be supported.

III. MIMO Expansion of CSL and YSL

Wireless systems extensively use MIMO methods to improve spatial coverage and efficiency. This section investigates their use in (possibly Y) CSL and also to expand wireless MIMO to yet more productive multi-antenna use.

Section III-A reviews wire pairs' wireless (or "common") modes, which essentially can double CSL's equivalent-wireline transmission capacity. Section III-B provides the frequency-scaled alternative to earlier multiplexing [39] [6] that generates a simple CSL-IF multiplexing enhancement. This alternative unblocks any spatial modes when there are an insufficient number of otherwise-high-frequency-bandwidth wireline links. Section III-C provides a more equal-fairness and usable alternative to the wireline link-bandwidth's spectral-spatial expansion (called "SF2SF" in [39]) to use MIMO methods fully. Section III-C also introduces a possibly cloud-managed CSL-RF+ that has "mid-MIMO" capabilities that can increase total bandwidth. The CSL-RF+ adds a precoder that is different from those introduced in [40] and that is instead optimum in the context of working with an existing cellular MIMO system. The optimum precoder's use is possible because of the frequency-scaling (or time-bursting equivalence). Section III-D progresses to an in-home multi-wire use of Wi-Fi, instead of cellular, that attempts to be well-matched to unlicensed spectrum use for in-home data transmission.

A. Use of Wireline's Wireless Modes

Each home's single twisted pair has 2 wires. Clearly, in wireless transmission cascaded with copper transmission, the possibility of sending a different wireless signal on each wire merits consideration, as in [6], [41]. Such systems would have larger wireless mutual and external crosstalk on both links, but nonetheless cellular MIMO principles apply directly to reduce this crosstalk.[30] The two transmissions, one initially on each wire, will be in the same band so necessarily then the external cellular system will perceive them as parallel, cellular, spatial streams. The MIMO cellular-baseband-processing system effectively removes the crosstalk that flows in the same direction. Full duplex operation is not possible because cancellation of echo (crosstalk) from ***other*** UE's uplink signals in the copper section is not possible physically in opposite directions. The common-mode's use

[30]One concern is wireline egress below 30 MHz, but experience with existing DSL deployments has shown the egress that results from high-frequency line imbalance (to common mode) can create egress power spectral densities of -70dBm/Hz that have not created a significant emissions issue and are widely deployed in many countries (whatever the applicable regulatory principles) without significant (efficiently manageable) disruption.

restores any CSL bandwidth lost to time-division directional changes because it effectively doubles (at least[31]) data rate. Similarly, the cellular (or equivalently Wi-Fi system) consequently uses 2 corresponding spatial streams. Traditionally such common-mode transmission in telephony was avoided because the much larger crosstalk reduces signal-to-noise ratio if considered as other users' noise relative to differential transmission using both wires for one differential signal. However, with cellular's or Wi-Fi's MIMO crosstalk reduction, such concern becomes minimal because that other-user noise is cancelled. CSL will still need to buffer (and frequency scale) downlink and uplink signals simultaneously to multiplex into downlink and upline transmission periods, just two such synchronized identical buffers occur in parallel (not shown but easily extrapolated in Figure 3), one for each wireline link. This section's remainder refers to a channel as one wireless channel, or resource block if multiple users present, whether or not it corresponds to a single channel on a wire pair or to one of 2 channels in parallel using the common mode. In the latter case, all Table III line/antenna performance data rates numbers can be approximately doubled without change of basic analysis and theory.

B. Exploitation of MU-MIMO and Frequency Scaling

A common frequency source for the (Y)CSL carriers allows different frequency-scaled channels on the same wireline link to use the same carrier on the wireless link (but on different spatial streams). YSL uses a clock-derivation scheme similar to that Figure 3's cellular system with just different counter values for Table II's various values.

Wireless' different spatial streams correspond to different time-division duplexed bursts of the CSL-IF and CSL-RF wireline link's transmissions. This spoofs space-time transmission only on the wireline link to create a transparent wireless multi-spatial-stream appearance on the overall cascaded link. CSL's same multi-user bursting also applies to a cellular system's different bands in inter-band carrier aggregation because the multi-user bursting accommodates the different streams (spatial or spectral). This concept improves upon the SF2SF in [39]. Figure 8a illustrates that a single wireline link has $m_{ST-CSL} = L$ channels where presently L is the number of spatial streams, with now a slightly expanded interpretation of the CSL's systems bandwidth index $m \rightarrow m_{ST-CSL}$. For the Wi-Fi example, $m_{ST-CSL} = 2$ could correspond to $L = 2$ spatial channels when the line length is sufficiently short (<800 m), which then supports the corresponding 50 MHz of bandwidth (with sampling rate 100 MHz) that shares both spatial streams through the single wireline link. Each time burst has identical format, just transmitted two times faster, or more generally $\frac{1}{T'''_{ST-CSL}} \rightarrow \frac{m_{ST-CSL}}{m} \cdot \frac{1}{T'''}$.

Figure 8a's ***m*-way** (Y)CSL has no wireline crosstalk between the different identically frequency-scaled time bursts. For example, a cellular system using two 20-MHz-wide spatial streams with $m = 16$ each would time-multiplex channels with a single (pre-frequency-scaled) IF carrier at 15.36MHz and $\frac{1}{T'''} = 61.44$ MHz because $m_{ST-CSL} = 2 \cdot 16 = 32$. The DAC sampling rate for the aggregate signal would be $\frac{8}{3} \cdot 2 \cdot 61.44$ MHz, with the extra factor of 2 representing the time-duplexing of the two spatial streams downlink in addition to 2 spatial streams uplink. Both downlink streams then ultimately occupy the same wireless frequency band between the CSL-RF and the user device(s), and thus also on the wireless link. Similarly, both upstream spatial streams occupy the same wireless frequency band. The CSL-RF thus uses the same carrier to (de)modulate separately each of the two spatial streams, one for each of the antennas. The spatial crosstalk will entirely occur in the wireless link. The cellular transmit-matrix-precoder processing shown (as a matrix multiply on the left in Figure 8a) leads to users' spatial separation at the two different home client devices. Again, the necessary MIMO signal processing already exists in modern cellular baseband transmitters, and thus need not change.

Cellular equipment that supports massive MIMO virtually assures that a number of spatial streams equal to the number of wireline frequency channels can be accommodated, because one of the wireline link's m_{ST-CSL} frequency-scaled time-burst channels then correspondingly supports each spatial cellular stream. These spatial streams can serve different users in MU-MIMO [42]. Indeed, the wireline link's burst-mode separation facilitates cellular's ability to orthogonalize spatial streams with respect to an all-wireless connection: That is, all MIMO signal processing power then applies to just the in-home wireless crosstalk rather than crosstalk on a longer length wireless channel with more potential for crosstalk interference.

More mathematically, following Figure 8a, $U = 2 \leq m_{ST-CSL} = L_w$ user devices use the cellular channel. A $U \times 1$ vector **s** contains the two downlink user-input streams intended for the two customer-premises-located users. The downlink precoder, implemented by the RAN as an $m \times U$ matrix multiply, has the $m \times 1$ vector output

$$\boldsymbol{x}_{d-bb} = Q_{d-ran} \cdot \boldsymbol{s}_d, \tag{11}$$

which enters the CSL-IF. Figure 8a presumes the RAN baseband has L spatial radios (which is typically true with L antennas so there is one radio/antenna). Instead of feeding antennas, these L connections feed the $m_{ST-CSL} = L$ CSL-IF burst-mode connections in the (complex baseband) time domain. The downlink wireline channel (including effects of any frequency scaling) has an output (with wireline noise organized into an $m \times 1$ vector $\mathbf{n}_{bb,fix}$)

$$\begin{aligned} \mathbf{y}_{d-bb,fix} &= H_{d-fix} \cdot \mathbf{x}_{d-bb} + \mathbf{n}_{d-bb,fix} \\ &= H_{d-fix} \cdot Q_{d-ran} \cdot \mathbf{s}_d + \mathbf{n}_{d-bb,fix}. \end{aligned} \tag{12}$$

The subscripts follow:

"d-bb" means downstream baseband,
"d-fix" means downlink wireline,
"d-air" means the wireless link, and
"d-ran" mean downlink radio-access node.

Similar subscript names apply uplink, with a "u" replacing the "d". The number of spatial channels $m_{5G-DFE} = L$

[31] Actually, such systems often experience more than 2x gain in practice because the attenuation of such common-mode signals is often less than differential-mode attenuation.

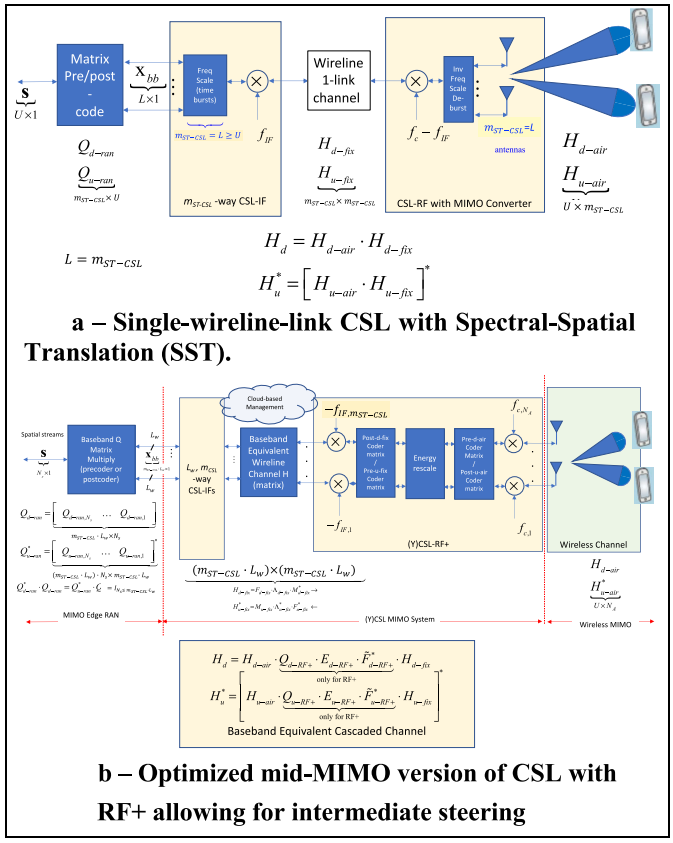

Fig. 8. (a) Single-wireline-link CSL with Spectral-Spatial Translation (SST). (b) Optimized mid-MIMO version of CSL with RF+ allowing for intermediate steering.

can exceed the number of users (and must be at least equal to the number of simultaneous users with linear precoding – nonlinear precoding[32] can accommodate smaller numbers of spatial-channels). The downlink wireless channel then has a $U \times 1$ vector output (with overall noise $\mathbf{n}_{bb}$ and each output component corresponding to the signal received at the user device)

$$\mathbf{y}_{d-bb} = H_{d-air} \cdot H_{d-fix} \cdot Q_{d-ran} \cdot \mathbf{s}_d + \mathbf{n}_{d-bb}. \quad (13)$$

With one user device and two antennas, the input $\mathbf{s}_d$ could continue to have two components, one for each spatial mode that reaches the 2-antenna device. In this case, H_{d-air} remains a 2×2 matrix, and there is additional cellular-device signal processing to decode the two modes and output the corresponding single-user data stream. The uplink processing reverses the flow in Figure 8a, which is the reason for Figure 8a's two-sided arrows. An easy uplink channel description is the forward path's transpose (conjugate transpose in complex baseband), recalling that the multiplication of a chain of matrices has a transpose that reverses its constituent matrices transposes' multiplicative order. The conjugate transpose also negates imaginary parts in defining/measuring the channel coefficients. Figure 8a uses this transpose notation, and the equation then directly follows as

$$\mathbf{y}_{u-bb} = Q_{u-ran}^* \cdot H_{u-fix}^* \cdot H_{u-air}^* \cdot \mathbf{s}_u + \mathbf{n}_{u-bb}. \quad (14)$$

As Figure 8a shows, the cellular RAN processing only sees the equivalent channels $H_d = H_{d-air} \cdot H_{d-fix}$ and $H_u^* = H_{u-fix}^* \cdot H_{u-air}^*$. The cellular signal processing determines the matrices Q_{d-ran} and Q_{u-ran}^* through QR factorization of the corresponding channel matrices, H_d and H_u, respectively.

C. MIMO Antenna Virtual Multiplication

Once Figure 8a is understood, Figure 8b envisions a more complex system. Figure 8b shows L_w wireline links that are available. In such a system, these wireline links carry up to $m_{ST-CSL} \cdot L_w$ spatial channels. The RAN baseband modulation must support the corresponding spatial channels. This support is already present in massive MIMO, but may well also be possible in most other RAN baseband systems, since often the key (CSL-averted) cost is only replication of the high-power RF amplifier and carrier modulator systems that would have otherwise been needed at the base station. Figure 8b illustrates a minimal increase in CSL-RF digital signal processing that significantly increases the overall-system capacity. The capacity increase then correspondingly can decrease the cost per supported user. Figure 8b's CSL may now experience crosstalk between the multiple wireline links on simultaneous bursts. In this wireline-crosstalk case, the CSL-RF could also simply remain the same as in Figure 8a, but Figure 8b shows an *optional* **mid-MIMO** CSL-RF+ processing that improves performance. Simple extension of Section II-C2's channel sounding[33] estimates the MIMO wireline H_d and H_u matrices. The mid-MIMO processing is not strictly necessary because the RAN baseband system's signal processing presumably has a sufficient number of spatial channels. However, when there is more than one device active at the customer premises, Figure 8b's[34] intermediate CSL-RF+ signal processing increases performance by improving the wireline-link performance that is essentially full MIMO (a single aggregate bit rate) and improved through channel singular value decomposition [43]. This processing maximizes the wireline link's aggregate data rate, decomposing it into a parallel channel set with highest performance and highest sum-data-rate possible. The outer cellular system then implements MU-MIMO. This is different from the precoders in [39] that instead precode the combination wireless/wireline, reducing performance, and then also possibly reducing the outer cellular MU-MIMO processing benefit that otherwise would have performed better. The wireless link outside the enhanced CSL+ then achieves a corresponding MU-MIMO optimum that uses the usual QR factorization [42]. A well-designed cellular system will inherently implement one of the unitary matrices of singular value decomposition, while the other will be in the CSL-RF+, which then amplifies appropriately. The CSL-RF+ can implement the final unitary matrix that

[32] Nonlinear precoding is not presently specified in any 3GPP nor Wi-Fi standards.

[33] All possible crosstalk transfers (any input to any output) are learned by the same procedure, which can be implemented simultaneously using methods in [31], Chapter 7.

[34] A CSL-RF+ includes a MIMO pre/post-coding within it.

completes the MU-MIMO signal processing for the wireless link, which derives from a QR factorization of only this final wireless link. With such processing, the number of antennas N_A at the CSL-RF+ output can exceed the number of spatial streams/limits at the RAN baseband system, further improving performance.

Mathematically, Equation (11) still holds except that the input contains N_S spatial streams that may each be for an individual user or can be combined to increase the data rates for a smaller number of users. The notational change from L to N_s emphasizes the now more general case than previously considered in Figure 8a. The RAN baseband precoder matrix Q_{d-ran} then becomes $m_{ST-CSL} \cdot L_w \times N_s$, which is a combination of a diagonal gain scaling of spatial-stream energies that is $m_{ST-CSL} \cdot L_w \times N_s$and the following $m_{ST-CSL} \cdot L_w \times m_{ST-CSL} \cdot L_w$ matrix, so (letting $m_{ST-CSL} \rightarrow m$ and $L_w \rightarrow L$ to simplify notation in (15))

$$Q_{d-ran} = \underbrace{\tilde{Q}_{d-ran}}_{mL \times mL} \cdot \underbrace{E_{d-ran}}_{\substack{mL \times N_x \\ \text{diagonal}}}, \tag{15}$$

for a linear precoder system. The optimum (nonlinear) precoder results in E_{d-ran} being generalized triangular and defining a dirty-paper precoder [42], but neither cellular nor Wi-Fi systems standards yet allow for this nonlinear-precoder form. Nonetheless, if the number of antennas is much larger than the number of streams, the performance loss that accrues to approximating the generalized triangular matrix by a diagonal in combination with the Q matrix is negligible [44]. Figure 8b simply shows the transmit matrix and not (15)'s decomposition. The downlink channel has singular value decomposition (SVD)

$$H_{d-fix} = F_{d-fix} \cdot \Lambda_{d-fix} \cdot M^*_{d-fix}, \tag{16}$$

as in Figure 8b. The best choice for the RAN baseband system (if it is working well, it will converge to this) has $\tilde{Q}_{d-ran} = M_{d-fix}$, as long as diagonal energy scaling adjoins the orthogonal matrix multiplication. In this case, the best mid-MIMO post H_{d-fix} matrix is $\tilde{F}_{d-fix} = F_{d-fix}$ and the wireline link will have been optimally diagonalized into its fundamental modes. These modes are scaled to appropriate energies before retransmission (there is still no decoding of cellular codes or messages). Again, this is optimal and thus different from the precoding methods in [39], which also attempt to approximate the solution to a well-known (without crosstalk cancellation) best spectrum assignment, sometimes known as optimum spectrum balancing [45]. The CSL-RF+ solutions in [5] and [6] find an optimum permutation matrix instead of a more generally complex-valued matrix, because those presumably are simpler to implement (apart from the frequency-scaled differences here). The approximate algorithms in [39] remain complex and are not necessary when the crosstalk cancellation can occur as with the methods proposed here (and furthermore [39]'s methods are not near optimum in this case). The wireless downlink has the generalized Q-R factorization ([31], Chapter 5)

$$H_{d-air} = \underbrace{R_{d-air}}_{U \times N_A} \cdot \underbrace{Q^*_{d-air}}_{N_A \times N_A}, \tag{17}$$

where the channel goes to the U user devices from N_A antennas. The number of antennas can be increased at this CSL-RF location if desired. This is typically an antenna-placement point with lower power and lower cost. The full massive MIMO effect will also be greater because these antennas are closer to the users and thus see reduced interference. The R_{d-air} matrix in (17) is often well approximated by a diagonal matrix in the $U \times U$ left columns (and zeros everywhere else). The downlink mid-MIMO precoder matrix for the wireless link is then $Q_{d-RF+} = Q_{d-air}$, and the gains on the wireless links[35] to each device are the diagonal elements of R_{d-air}. The overall downlink system then has channel

$$\begin{aligned} H_d \cdot Q_{d-ran} &= H_{d-air} \cdot \underbrace{Q_{d-RF+} \cdot E_{d-RF+} \cdot \tilde{F}^*_{d-RF+}}_{\text{only for RF+}} \cdot H_{d-fix} \\ &\quad \cdot Q_{d-ran} \\ &\cong E_{d-air} \cdot E_{d-RF+} \cdot E_{d-ran}, \end{aligned} \tag{18}$$

where $E_{d-air} = diag(R_{d-air})$ and the diagonals have no more than $\min\{N_S, N_A, U\}$ non-zero elements. The uplink system similarly has

$$\begin{aligned} &[H_{u-air} \cdot Q_{u-ran}]^* \\ &= \left[H_{u-air} \cdot \underbrace{Q_{u-RF+} \cdot E_{u-RF+} \cdot \tilde{F}^*_{u-RF+}}_{\text{only for RF+}} \cdot H_{u-fix} \cdot Q_{u-ran} \right]^* \\ &= E_{u-ran} \cdot E_{u-RF+} \cdot E_{u-air}. \end{aligned} \tag{19}$$

Certain fully optimum solutions will find adjusted E matrices when these factors absorb into the Q matrices and thus found adaptively through minimum-mean-square-error adaptive algorithms.

The CSL-RF+ use effectively enables the spectral-spatial translation to increase the number of antennas without changing the existing RAN. The computations (SVD, QR, etc.) need not be real-time and can be implemented in the cloud.

D. Residential YSL

The basic YSL architecture could follow that of cellular as in Section II-E. However, the value of sending Wi-Fi signals on wires from the internet service provider's nearest edge point may be dubious compared to sending cellular signals. Instead, YSL's use may make better practical sense within customer premises. In particular, Wi-Fi MAP or mesh-point (MP) systems have digital[36] relays within the customer premises. These systems reduce bandwidth efficiency, because they use two different Wi-Fi channels for the same data into and out of each MAP or MP relay, to improve coverage. The bandwidth loss can be significant because of collisions between multiple Wi-Fi networks and users within the access point's vicinity. Most customer premises however do have wires. There are

[35]SVD calculation of Q_{d-air} and R_{d-air} require knowledge of H_{d-air} and the CSL-RF+ must observe passing training downlink sequences for the wireless link and corresponding responses from the client device that provide the equivalent of H_d. Then $H_{d-air} = H^+_{d-fix} \cdot H_d$, where the superscript of $+$ means pseudo-inverse on the fixed-channel matrix.

[36]Digital here means a full Wi-Fi demodulator/decoder and modulator/re-encoder exists within the MAP or MP.

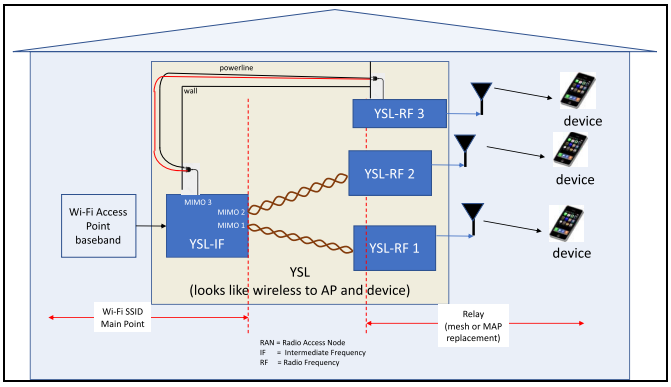

Fig. 9. YSL residential architecture using in-home wiring to some mesh/multi-AP points.

often multiple in-home phone lines: an RJ-11 phone jack and cable for instance has two pairs of wires connected within it and indeed these often are supported by the wiring within the home. The home may also have power lines, possibly coaxial cable, and maybe other wiring systems, although these will typically not terminate on the final end device. Instead these wireline links terminate at various customer-premises locations. The YSL system then places Section II-D's simple YSL-RF converter at some or all these locations, typically at far lower cost than a full MP or MAP.

Figure 9 illustrates a residence that uses wireline connectivity to (all or most) different RF sites within the home. Shown are two twisted pairs and one power line. However, other cabling like coaxial cable could also be used if present. The 3 YSL-RF devices shown are of the same type used earlier in YSL. This is essentially a distributed antenna system [14] in basic architecture. The YSL-RF devices though are simple low-cost analog modulators (along with digital control channel) not full MAP or MP devices. Such a system exploits existing wires to (at least) place "repeaters" at many locations that would extend coverage (in addition to additional wireline-inaccessible locations that still require wireless relay connection). Such a proposed system's performance is, at a minimum, better for each wireline connection that saves a wireless channel for wireless use. Since the short connections within the home can support as many as 8 Wi-Fi channels, the performance improvement is consequently very substantial. For instance, a Wi-Fi 6 (802.11ax) transmission that uses a significant portion of the 5 GHz band with relays will occupy the entire band for the length of its transmission because there are only two such channels at 5 GHz. YSL could then reduce the frequency-band occupancy with lower power signals at the wires' south ends. Figure 9's wireline portion also exploits the MIMO spatial channels because any spatial interference between signals will be confined to the wireless links and the wireline's spatial streams will be in different bursts. If there is crosstalk between the in-home wires, then indeed Wi-Fi's MIMO processing power will in part need to address it. This allows more complete use of transmit energy on each such spatial stream and further increases performance. Finally, this architecture uses only one Wi-Fi channel, not two, thus avoiding the mesh-points' and multiple-access points' most important deficiency.

IV. YSL, Ethernet, MESH, and Enterprise

Enterprise Wi-Fi's use in small companies, branch offices of large companies, schools, apartment complexes, malls, and similar homogenous-access opportunity often requires coordinated-mesh control of MAPs or MPs. Such enterprise applications often also have internal Ethernet cabling. The Ethernet cable often connects a router to multiple Wi-Fi APs, but this does not by itself resolve Wi-Fi spectrum-contention issues of the APs' common shared channels. Solutions increasingly emerge where many or all AP's (or the slightly reduced MP forms) connect wirelessly with some coordinated channel selection, in particular when using the MP's or AP's to relay signals to points too distant from a master AP for successful connection, that is to "cover" the enterprise. Successful coverage often allocates different channels (even if the same SSID is used) to different enterprise-space partitions to avoid excessive collision. While coverage improvement can occur with the MAPs or MPs, overall network throughput may be consequently well below best possible levels. More desirable is a more coordinated Wi-Fi system, effectively a "massive-AP" functionality that covers all points but also has efficient spectrum use. This section describes how Ethernet cabling offers an opportunity to implement this massive-AP functionality. Ericsson's "Radio Dot System" (RDS) [46] introduced an alternative more limited system (without the frequency-scaling and consequent aversion of collision issues) that uses 3GPP's centralized control.

Section IV-A discusses simple YSL-Ethernet solutions using a single Ethernet cable as the first connection (instead of the telephone lines as in Sections II and III), again with simple devices and little (or no) need for full AP's at the Ethernet terminations. Instead, the solution simply uses YSL-RFs to translate AP signals on the Ethernet-cable wires' south outputs into wireless signals. Section IV-A considers a single AP and a single Ethernet cable that contains 4 twisted pairs (or 8 wires). Section IV-B uses Section III's multi-way C(Y)SL-IF to support several APs' signals on a single Ethernet cable, presuming the coordination of 4 physically co-located AP's in a **YSL-MAP**. The name "YSL-MAP" (YSL – multi-access point) adds the term YSL to MAP to imply that all APs are in the same physical location (unlike most MAP systems today or mesh MP systems), even though they appear from a functional/virtual standpoint at the sound ends of the Ethernet cables. This system greatly enhances use of multiple-antenna-capable AP's (with respect to a traditional mesh system). Section III-C's CSL-RF+ optionally enhances performance further, now as a **YSL-RF**+. Section IV-C addresses a more sophisticated multi-user YSL-RF capability that employs multiple coordinated YSL-MAPs on an Ethernet cable system throughout an enterprise, yet further enhancing enormously Wi-Fi connectivity possibilities. These systems will add multiple YSL-RF+ capabilities. Throughout, this section suggests the possibility of a cloud-based externally managed software system (that need not be in the AP's themselves) that renders

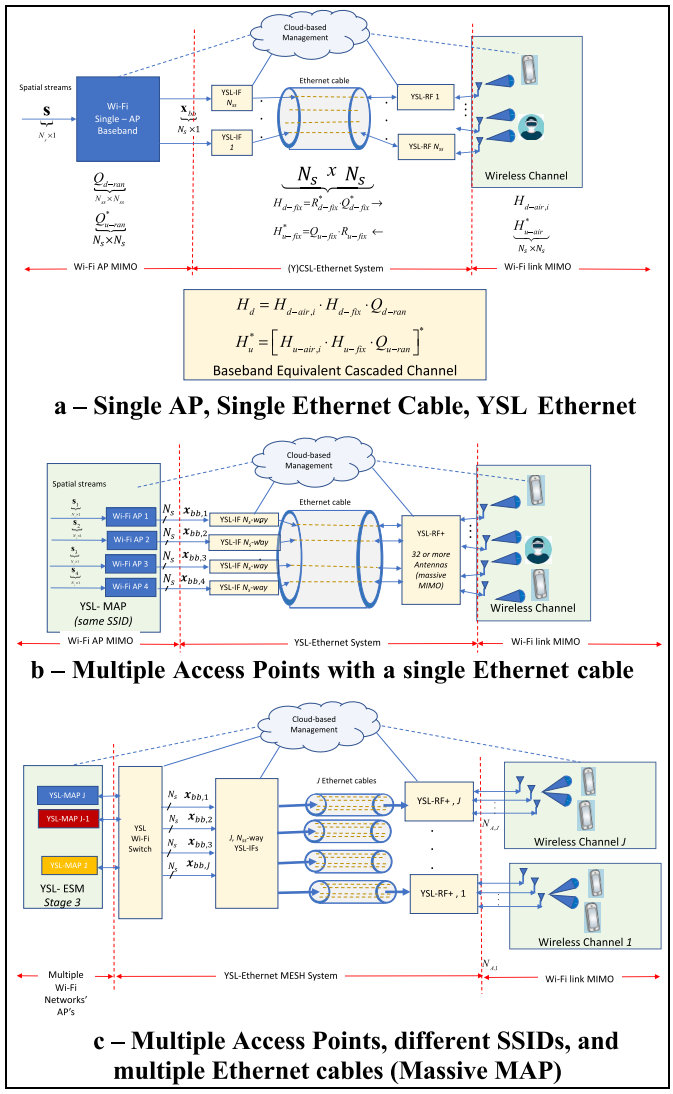

Fig. 10. (a) Single AP, single ethernet cable, YSL-ethernet. (b) Multiple access points with a single ethernet cable. (c) Multiple access points, different SSIDs, and multiple Ethernet cables (Massive MAP).

the overall coordination effectively independent of the Wi-Fi APs (apart from the access to the baseband signals prior to RF modulation as is the case throughout this article). Such systems may allow maximum legacy compatibility with existing Wi-Fi systems' standards.

A. 1 Single AP, Single Ethernet Cable, YSL-Ethernet

While phone wires exist in most small businesses, typically internet connectivity is through Ethernet cabling (cat5, 6, 7, …) from a server/IT location ("closet") to working locations throughout the building/complex. Ethernet cable lengths are less than 100m, and therefore allow up to $m_{Enet} = 8$. Thus, each ethernet cable pair (or with Section III-A's techniques, each of the 8 wires) can readily support a single 50-200 MHz-wide signal (the maximum bandwidth allowed in Wi-Fi 6 for instance in the bands below 7 GHz is 160 MHz, so frequency scaling of YSL is feasible because YSL's bandwidth is 200 MHz with $D = 1.25x$). Thus, a single Ethernet cable readily supports up to $N_s \leq 8$ spatial streams. Figure 10a's YSL-Ethernet shows this support for 4 links (presumably use of all 4 twisted pairs in differential mode) and thus implies $N_s = 4$. The 4 spatial streams (up to 160 MHz wide each) flow downlink (and corresponding return uplink) at IF between the YSL-IF and YSL-RF. The YSL-RF's are separate, one for each link through the Ethernet cable. Each has a single antenna and supports devices within the wireless coverage of the YSL-RF. Any and all MIMO processing is baseband in this Wi-Fi AP system. The various transfer-function matrices appear in Figure 10a, as in Section III's mathematical description and have not changed with respect to earlier figures. The wireline link now contains all the Ethernet cable's pairs. These Ethernet cables also better support YSL's high frequency bands than lower-grade cables. There will be crosstalk between these pairs, and so the Wi-Fi baseband MIMO processing also accommodates this crosstalk along with the cascaded wireless link's crosstalk. Thus, Wi-Fi signals on the same channel's different spatial streams must correspond to coincident YSL-Ethernet transmission's frequency-scaled bursts.

The cloud-management system allows for CSL-IF and CSL-RF power-level adjustment and carrier-frequency choices at the CSL-RF in ways that may be completely transparent to the Wi-Fi AP and client devices, which simply see a standard Wi-Fi channel. In effect, the CSL-IF and CSL-RF become low-cost internet devices ("things") in the simplest enterprise case of YSL-Ethernet. These devices do not decode nor view personal information, but simply allocate efficiently the enterprise's unlicensed spectra. Optionally, it would be possible for a compatible Wi-Fi AP, and possibly also a compatible Wi-Fi device, to provide information to the cloud management, as well as accept policy advice or controls from it (see [37]), as in Figure 10a's dashed lines. While simple in implementation and concept, and likely easily deployed, the YSL-Ethernet suggests yet more powerful combinations as in Sections IV-B and IV-C.

B. Multi AP, Single Ethernet Cable, YSL-Ethernet

Figure 10b's YSL MAP shows a coordinated set of 4 APs. The YSL MAP exploits a single Ethernet wire-pair's full bandwidth to carry a single AP's full set of spatial streams. This single pair (as a link) can carry at least 4-8 160-MHz wide channels. A two-link (using each wire with respect to ground as in Section III-A) could carry all 8. The CSL-IF has now expands to Section III-B's and III-C's N_s – way version to burst-multiplex by frequency scaling all spatial components on the single wireline link. Figure 10b's system with 4 wireline links supports 4 APs. These 4 APs may be coordinated by an enterprise controller, but perhaps more easily and flexibly handled by leaving them as independent APs while cloud-based management instead provides the resource-management policy of carrier frequencies and spatial modes [37]. Interesting here with a single Ethernet cable is that the YSL-RF can now become a YSL-RF+ (See Section III-C) that allows increase of the number of antennas (up to 32 then for the existing Wi-Fi system[37]), but YSL-RF+ places the additional antennas so as to expand Wi-Fi's ability

[37]The AP may need to select the best 8 from the 32.

to support multiple devices in limited crowded space, as may likely occur in an enterprise application. Such a system could easily outperform even the best of 5G femtocell systems that are contemplated for enterprise use today (of course, a YSL-Ethernet system on licensed spectra that mirrors the Figure 10b's design might gain the same advantages).

C. Multi AP, Multiple Ethernet Cable, YSL-Ethernet

Figure 10c expands further Section IV-B's concepts to multiple Ethernet cables, as is very likely to be the infrastructure in an enterprise application. These cables are, at the client side, in multiple physical locations within the enterprise. Multiple YSL-MAPs, in what could be called a "massive MAP," appear at the "IT-Closet" (left) side of Figure 10c. These each could connect to their own N_s-way CSL-IF, but Figure 10c's Massive MAP adds a new Wi-Fi switch to address coverage problems. One issue in Wi-Fi coverage is that "another AP" or SSID is physically closer to the target client device than the one with the correct SSID for access. The switch allows a virtual physical relocation of any APs to any of the multiple CSL-RF+ points (on one channel, several, or all). There are J YSL-MAPs shown to cover all J of the physical Ethernet cables going to different physical locations. Switching should avoid wireline-link crosstalk introduction between two different AP's for uncoordinated baseband MIMO processing. All MAPs are all synchronized as in Section II. The MAPs could again use cloud-based management of the now coordinated set to avoid change to the existing Wi-Fi. Methods such as the Stage 3 ESM of [37] apply to such a configuration to provide very accurate signal delivery to specific client-locations, anywhere within the range of any of the enterprise's Ethernet cable termination locations.

V. Conclusion

Reuse of the existing wireline infrastructure (phone lines, Ethernet cables, powerlines, coaxial cables, and possibly fiber) can magnify the coverage, efficiency, and opportunity for wireless systems like cellular (5G or even existing 4G) as well as Wi-Fi. The re-use of cellular licensed-wireless methods seems best suited to the existing large base of twisted-pair connections to create many more effective (lower power, less interference) cell-tower equivalents closer to users and inside homes, expanding cost-effectively coverage and speeds. The re-use of Wi-Fi methods seems best suited to enterprise applications where an existing base of Ethernet cable exists and can be exploited. Either of course can be used in the other infrastructure as well from a fundamental standpoint. The intermediate super-heterodyning concept of IF and RF can enable very low-cost proliferation and allow cloud-based control to enhance existing standardized infrastructure with no compromise of personal-information in basic operation. These (Y)CSL/Ethernet systems may well provide a good solution to the increasing need for more cost-effective wireless deployment so that the promise of a highly connected wireless future can advance with much less economic risk.

Acknowledgment

The authors would like to thank Prof. Umberto Spagnolini for his extensive and helpful comments.

References

[1] J. Gambini and U. Spagnolini, "Radio over telephone lines in femtocell systems," in *Proc. 21st Annu. IEEE Int. Symp. Pers., Indoor Mobile Radio Commun.*, Sep. 2010, pp. 1544–1549.

[2] J. Gambini and U. Spagnolini, "Wireless over cable for femtocell systems," *IEEE Commun. Mag.*, vol. 51, no. 5, pp. 178–185, May 2013.

[3] S. H. R. Naqvi, A. Matera, L. Combi, and U. Spagnolini, "On the transport capability of LAN cables in all-analog MIMO-RoC fronthaul," in *Proc. IEEE Wireless Commun. Netw. Conf. (WCNC)*, Mar. 2017, pp. 1544–1549.

[4] U. Spagnolini and J. Gambini, "Equipment for femtocell telecommunications system," Eur. Patent EP 2 540 134 B1, Oct. 19, 2016.

[5] A. Matera and U. Spagnolini, "Analog MIMO radio-over-copper downlink with space-frequency to space-frequency multiplexing for multi-user 5G indoor deployments," *IEEE Trans. Wireless Commun.*, vol. 18, no. 5, pp. 2813–2827, May 2019.

[6] U. Spagnolini, "Transporting radio signals using a low frequency band over copper cables," U. S. Patent 10 333 584, Aug. 8, 2016.

[7] U. Spagnolini, J. Gambini, and M. Arigossi, "Equipment for femtocell telecommunications system," U. S. Patent 9 107 203 B2 Feb. 24, 2011.

[8] Y. Huang *et al.*, "LTE over copper—Potential and limitations," in *Proc. IEEE 26th Annu. Int. Symp. Pers., Indoor, Mobile Radio Commun. (PIMRC)*, Aug. 2015, pp. 1339–1343.

[9] M. Berg, E. L. Madeiros, A. M. Calalconte, and I. Almeida, "Methods and devices for adapting load on a fronthaul network," European Patent Appl. Patent WO 2 018 093 301, Nov. 16, 2016.

[10] C. Lu, T. Elmar, J. Osterling, P.-E. Eriksson, and R. Bergquist, "Methods and network nodes for communication between a first network node and a second network node over A twisted pair wire," U.S. Patent 9 918 327, May 2, 2016.

[11] J. Botha, *The FOA Outside Plant Fiber Optics Construction Guide*. Santa Monica, CA, USA: Fiber Optics Association, 2019.

[12] Handelsblatt Today. *Mobile Carriers' Next Challenge: Finding the Money for 5G*. Feb. 23, 2018. [Online]. Available: https://www.handelsblatt.com/today/companies/200-300-billion-mobile-carriers-next-challenge-finding-the-money-for-5g/23581238.html?ticket=ST-48284083-y7lUF0e0vtVy0fr6CtsD-ap3

[13] *Technical Specification 101 548 - European Requirements for Reverse Powering of Remote Access Equipment, V2.1.1*, Standard ETSI TS 101 548, 650 Route des Lucioles F-06921 Sophia Antipolis Cedex–FRANCE, European Telecommunications Standards Institute (ETSI) Sep. 2016.

[14] H. Hu, Y. Zhang and J. Luo, *Distributed Antenna Systems: Open Architecture for Future Wireless Communication*, Boca Raton, FL, USA: Auerbach Pulications, 2019.

[15] A. B. Ericsson, *Huawei Technologies Co. Ltd, NEC Corporation and Nokia*. Bengaluru, Karnataka: Common Public Radio Interface, CPRI, 2017.

[16] 5G PPP. (Jun. 30, 2016). *5G-Xhaul—Dynamically Reconfigurable Optical-Wireless Backhaul/Fronthaul with Cognitive Control Plane for Small Cells and Cloud-RANs*. Horizon 2020 Program of European Commission. Accessed: May 7, 2019. [Online]. Available: https://www.5g-xhaul-project.eu/publication_deliverables.html

[17] I. A. Alimi, A. L. Teixeira, and P. P. Monteiro, "Toward an efficient C-RAN optical fronthaul for the future networks: A tutorial on technologies, requirements, challenges, and solutions," *IEEE Commun. Surveys Tuts.*, vol. 20, no. 1, pp. 708–769, 1st Quart., 2018.

[18] J. M. Cioffi, K. J. Kerpez, C. S. Hwang, and I. Kanellakopoulos, "Terabit DSLs (invited paper)," *IEEE Commun. Mag.*, vol. 56, no. 11, pp. 152–159, Nov. 2018.

[19] R. Shrestha, K. Kerpez, C. S. Hwang, M. Mohseni, J. M. Cioffi, and D. M. Mittleman, "A wire waveguide channel for terabit-per-second links," *Appl. Phys. Lett.*, vol. 116, no. 13, Mar. 2020, Art. no. 131102.

[20] F. Ling, *Synchronization in Digital Communications*. Cambridge, U.K.: Cambridge Univ. Press, Jun. 2017.

[21] G. M. Garner, "IEEE 1588 version 2," in *Proc. ISPCS*, Ann Arbor, MI, USA, vol. 24, Sep. 2008.

[22] *Long Term Evolution—Release 16*, Standard 3GPP TR 21.916, Release Description, Release, Dec. 2019.

[23] E. Perahia and R. Stacey, *Next Generation Wireless LANS: 802.11n and 802.11ac*, 2nd ed. Cambridge, U.K.: Cambridge Univ. Press, 2013.
[24] L. Miller, *Carrier Aggregation for Dummies*. Hoboken, NJ, USA: Wiley, 2016.
[25] A. Zaidi, F. Athley, J. Medbo, U. Gustavsson, G. Durisi and X. Chen, *5G Physical Layer Principals, Models, and Technology Components*. London, U.K.: Academic, 2018.
[26] T. Starr, J. M. Cioffi and P. J. Silverman, *Understand Digital Subscriber Line Technology*. Upper Saddle River, NJ, USA: Prentice-Hall, 1999.
[27] S. Wicker, *Error Control Systems for Digital Communication and Storage*. Upper Sadde River, NJ, USA: Prentice-Hall, 1995.
[28] Wikipedia. (Jan. 9, 2020). *High-Level Data Link Control*. Accessed: Feb. 7, 2020. [Online]. Available: https://en.wikipedia.org/wiki/High-Level_Data_Link_Control
[29] J. M. Cioffi, P. S. Chow, and K. J. Kerpez, "Optimum equivalent loading in multi-dimensional transmission," *IEEE Open J. Commun. Soc.*, vol. 1, pp. 681–699, 2020.
[30] H. Lee, S. Vahid, and K. Moessner, "A survey of radio resource management for spectrum aggregation in LTE-advanced," *IEEE Commun. Surveys Tuts.*, vol. 16, no. 2, pp. 745–760, 2nd Quart., 2014.
[31] J. M. Cioffi. (Jul. 3, 2020). *Digital Data Transmission*. Accessed: Jul. 3, 2020. [Online]. Available: http://web.stanford.edu/group/cioffi/book/
[32] A. El Gamal, M. Mohseni, and S. Zahedi, "Bounds on capacity and minimum energy-per-bit for AWGN relay channels," *IEEE Trans. Inf. Theory*, vol. 52, no. 4, pp. 1545–1561, Apr. 2006.
[33] *Improved Impulse Noise Protection for Digital Subscriber Line (DSL) Transceivers*, document G.998.4, Geneva, Switzerland, International Telecommunications Union Mar. 27, 2019.
[34] M. M. T. Chowdhury. (2013). *Hybrid Automatic Repeat Request in LTE*. Rochester Institute of Technology. Accessed: Aug. 31, 2019. [Online]. Available: https://pdfs.semanticscholar.org/6b24/754829400d44e637c138e9dd1da7d323cd1f.pdf
[35] T. Starr, J. M. Cioffi and P. J. Silverman, *Understanding Digital Subscriber Line Technology*. Upper Saddle River, NJ, USA: Prentice-Hall, 1999.
[36] T. Starr, M. Sorbara, J. M. Cioffi and P. J. Silverman, *DSL Advances*. Upper Saddle River, NJ, USA: Prentice-Hall, 2003.
[37] J. M. Cioffi, C.-S. Hwang, and K. J. Kerpez, "Ergodic Spectrum Management (ESM), invited paper," *IEEE Trans. Commun.*, vol. 68, no. 3, pp. 1794–1821, Mar. 2020.
[38] *Standard for a Convergent Digital Home Network for Heterogeneous Technologies*, Standard P1905-2013, P1905 Working Group 2013.
[39] A. Matera, L. Combi, S. H. R. Naqvi, and U. Spagnolini, "Space-frequency to space-frequency for MIMO radio over copper," in *Proc. IEEE Int. Conf. Commun. (ICC)*, May 2017, pp. 1–6.
[40] E. Lins de Maderios, P.-E. Eriksson, Y. Huang, and C. Lu, "Methods and nodes of a wireless communication network for mitigating crosstalk in a distributed base station system," European Patent EP 3 257 165 B1, Nov. 2, 2015.
[41] S. Jagannathan, V. Pourahmad, K. Seong, J. M. Cioffi, M. Ouzzif, and R. Tarafi, "Common-mode data transmission using the binder sheath in DSL," *IEEE Trans. Commun.*, vol. 57, no. 3, pp. 831–840, Feb. 2009.
[42] R. W. J. Heath and A. Lozano, *Foundations of MIMO*. Cambridge, U.K.: Cambridge Univ. Press, 2019.
[43] S. Kasturia, J. T. Aslanis, and J. M. Cioffi, "Vector coding for partial response channels," *IEEE Trans. Inf. Theory*, vol. 36, no. 4, pp. 741–762, Jul. 1990.
[44] E. Bjornson, E. G. Larsson, and T. L. Marzetta, "Massive MIMO: Ten myths and one critical question," *IEEE Commun. Mag.*, vol. 54, no. 2, pp. 114–122, Feb. 2016.
[45] R. Cendrillon and M. Moonen, "Iterative spectrum balacing for digital subscriber lines," in *Proc. Iternational Conf. Commun.*, Seoul South Korea, May 2005, pp. 1937–1941.
[46] C. Lu *et al.*, "Connecting the dots: Small cells shape up for high-performance indoor radio," *Ericsson Rev.*, vol. 19, pp. 38–45, Dec. 2014.
[47] M. Aldababsa, M. Toka, S. Gökçeli, G. K. Kurt, and O. Kucur, "A tutorial on nonorthogonal multiple access for 5G and beyond," *Wireless Commun. Mobile Comput.*, vol. 2018, pp. 1–24, Jun. 2018.
[48] J. M. Cioffi, K. Kerpez, C. S. Hwang, and I. Kanellakoupolous, "Roadmap to terabit DSLs," in *Proc. TNO Conf.*, Hague, The Netherlands, Jun. 2018, pp. 1–23.
[49] P. Spruyt, "Achievements & advances in next-gen copper access," in *Proc. TNO*, Hague, The Netherlands, Jun. 2019, pp. 1–31.
[50] Ericsson AB. (2015). *Huawei Technologies Co. Ltd, NEC Corporation, Alcatel Lucent, and Nokia Networks*. Common Public Radio Interface (CPRI) Specification 7.0. [Online]. Available: http://www.cpri.info/downloads/CPRI_v_7_0_2015-10-09.pdf

John M. Cioffi (Fellow, IEEE) was born in Illinois. He received the B.S.E.E. degree in 1978 and the Ph.D. degree in EE, Stanford, in 1984. He has been a Professor of EE, Stanford, since 1986. He has published more than 600 articles and has more than 100 heavily licensed patents. He was the Marconi Fellow in 2006 and a member of U.S. National in 2001 and the U.K. Royal Engineering Academies in 2009. He is an Emeritus. He is a Founder Amati 1991 (1997 purchased by TI), the Chairman, and a CEO ASSIA Inc. His research interest includes high-performance digital transmission. His awards include the IEEE AG Bell in 2010 and the Kirchmayer in 2014 and Medals includes the Member Internet in 2014 and the Consumer-Electronics in 2018, and the Halls of Fame.

Chan-Soo Hwang (Senior Member, IEEE) received the Ph.D. degree in EE from Stanford University in 2007. From 1999 to 2010, he worked on VDSL and 4G/5G wireless communications with Samsung Electronics. Since 2010, he has been developing machine-learning techniques for optimizing DSL, Wi-Fi networks, and sensor systems at ASSIA and Tinoq. He received the Best Paper Awards from the IEEE ICC 2006 and 2008. His research interests include communication systems, signal processing, and machine learning.

Ioannis Kanellakopoulos (Fellow, IEEE) received the Ph.D. degree in EE from the University of Illinois at Urbana–Champaign. He is currently a Technology Consultant and an Expert Witness at Oraton Consulting. As a Consulting Chief Scientist for ASSIA, Inc., he provides intellectual property and technology-strategy services. His past positions include CTO at Actelis Networks, Chief Scientist at Voyan Technology, and Professor and Vice Chair in the UCLA Department of Electrical Engineering. His awards include the IEEE CSS George S. Axelby Best Paper Award and the AACC Donald P. Eckman Award.

Jisung Oh (Member, IEEE) received the B.S. and M.S. degrees in control and instrumentation engineering from Seoul National University, South Korea, in 1994 and 1996, respectively, and the Ph.D. degree in electrical engineering from Stanford University, Stanford, CA, USA, in 2005. He started his career at Samsung Electronics as a Communications Systems Engineer in 1996 and worked in multiple business divisions including digital TV, mobile handset, and telecommunication networks. He led mmWave core technology development for 5G network from 2016 to 2018. Since 2019, he has been with ASSIA Inc., as the Vice President of wireless development and is in charge of cloud-based wireless network management.

Ken J. Kerpez (Fellow, IEEE) received the Ph.D. degree in EE communications from Cornell University in 1989. He worked at Bellcore and Telcordia, for 20 years, where he has been working at ASSIA for nine years. He became an IEEE Fellow in 2004 for his contributions to broadband technology and standards. He has published nearly a hundred articles and authored over eight hundred standards contributions. He has many years of experience working on communications systems and networks of all sorts, including DSL, fiber access, home networks, wireless systems, broadband service assurance, IP QoS, triple-play services, virtualization, Wi-Fi, and 5G.